Journal of Medicinal Chemistry

Article

Discovery of 2-Indole-acylsulfonamide Myeloid Cell Leukemia 1 (Mcl-1) Inhibitors Using Fragment-Based Methods

Nicholas F Pelz, Zhiguo Bian, Bin Zhao, Subrata Shaw, James C. Tarr, Johannes Belmar, Claire Gregg, DeMarco V. Camper, Craig M. Goodwin, Allison L. Arnold, John L. Sensintaffar, Anders Friberg, Olivia W. Rossanese, Taekyu Lee, Edward T Olejniczak, and Stephen W. Fesik

J. Med. Chem., **Just Accepted Manuscript** • DOI: 10.1021/acs.jmedchem.5b01660 • Publication Date (Web): 15 Feb 2016

Just Accepted

ACS Publications

Journal of Medicinal Chemistry is published by the American Chemical Society. 1155 Sixteenth Street N.W., Washington, DC 20036

Discovery of 2-Indole-acylsulfonamide Myeloid Cell Leukemia 1 (Mcl-1) Inhibitors Using Fragment-Based Methods

*Nicholas F. Pelz[#], Zhiguo Bian[#,], Bin Zhao, Subrata Shaw, James C. Tarr, Johannes Belmar, Claire Gregg, DeMarco V. Camper, Craig M. Goodwin, Allison L. Arnold, John L. Sensintaffar, Anders Friberg^, Olivia W. Rossanese[+], Taekyu Lee, Edward T. Olejniczak, and Stephen W. Fesik**

Department of Biochemistry, Vanderbilt University School of Medicine, 2215 Garland Avenue, 607 Light Hall, Nashville, Tennessee 37232-0146, USA

[#] These authors contributed equally to this work.

KEYWORDS:

Fragment-based screening; apoptosis; cancer; Mcl-1; drug discovery

ABSTRACT

Myeloid cell leukemia-1 (Mcl-1) is a member of the Bcl-2 family of proteins responsible for the regulation of programmed cell death (PCD). Amplification of Mcl-1 is a common genetic aberration in human cancer whose overexpression contributes to the evasion of apoptosis and is one of the major resistance mechanisms for many chemotherapies. Mcl-1 mediates its effects primarily through interactions with pro-apoptotic BH3 containing proteins that achieve high affinity for the target by utilizing four hydrophobic pockets in its binding groove. Here we describe the discovery of Mcl-1 inhibitors using fragment based methods and structure-based design. These novel inhibitors exhibit low nanomolar binding affinities to Mcl-1 and greater than 500-fold selectivity over Bcl-xL. X-ray structures of lead Mcl-1 inhibitors when complexed to Mcl-1 provided detailed information on how these small-molecules bind to the target, and were used extensively to guide compound optimization.

INTRODUCTION

The ability of tumor cell populations to increase in number is not only dependent upon their rate of proliferation, but also upon their rate of attrition[1, 2]. Apoptosis, or programmed cell death (PCD), is a major source of cell attrition, and the evasion of apoptosis is a hallmark of cancer.[3, 4] The cell's decision to undergo apoptosis is regulated by a balance of pro-apoptotic and anti-apoptotic proteins that respond to various extracellular and intracellular stress factors, including oxygen deprivation, DNA damage, oncogene signaling, and cytotoxic drugs[1]. In cells, stress can induce the oligomerization of the pro-apoptotic proteins Bax and Bak, which leads to the permeabilization of the outer membrane of the mitochondrion, release of cytochrome C, and the initiation of caspase-dependent apoptosis[5]. Anti-apoptotic proteins such as Bcl-2, Bcl-xL, Bcl-w, Bcl-A1 (Bfl-1), and Mcl-1 guard against PCD by sequestering their pro-apoptotic relatives resulting in the inhibition of apoptosis[2, 6]. Overexpression or up-regulation of the anti-apoptotic Bcl-2 family proteins enhance cancer cell survival and cause the resistance to a variety of anti-cancer therapies[7]. Consequently, targeting the Bcl-2 family of proteins represents an attractive strategy for cancer drug discovery[8, 9]. Indeed, this strategy was validated by the discovery of Navitoclax (ABT-263), a potent inhibitor of Bcl-xL, Bcl-w, and Bcl-2[10]. In addition, a potent Bcl-2 selective inhibitor, Venetoclax (ABT-199), was recently discovered to avoid the thrombocytopenia observed by inhibiting Bcl-xL[11]. Venetoclax is currently in Phase III clinical trials[12].

Early leads targeting another important member of the family, Mcl-1, have also recently been reported.[13-18] Mcl-1 is of considerable interest because it is the major cause of resistance to Navitoclax, Venetoclax,[19, 20] as well as the widely prescribed anti-cancer

agents paclitaxel, vincristine[21], and gemcitabine[22]. Also, Mcl-1 amplification is one of the most common genetic aberrations observed in human cancers[23], and its overexpression[24] is implicated in a variety of cancers, including leukemia, melanoma, lung, breast, prostate, pancreatic, ovarian, and cervical cancers.

The Bcl-2 family of proteins, including Mcl-1, are inherently difficult to target because they exert their effects through a large protein-protein interface[25]. The BH3 regions of pro-apoptotic proteins interact with Mcl-1 utilizing four hydrophobic pockets in Mcl-1's binding groove[26, 27]. The BH3 region of Bcl-2 family proteins is an amphipathic helix containing four key hydrophobic residues (H1-H4: L210, L213, V216, V220 in Mcl-1 BH3 PDB_ID: 3MK8[28] or ILIF in Bim BH3 PDB_ID: 2NL9[29]) that are essential for binding to the corresponding active site pockets P1-P4 of the anti-apoptotic Bcl-2 family members[27]. Mutating any of these four residues to alanine significantly reduces binding to Mcl-1. For example, for the Mcl-1 BH3 peptide, an 800 fold decrease is observed by mutating the H2 residue, L213 to an alanine, while mutating H3 (V216A) or H4 (V220A) causes nearly a 100 fold drop in binding affinity to Mcl-1[28].

We previously described the discovery of small-molecule Mcl-1 inhibitors that primarily bind to the P2 pocket[13, 16]. In order to obtain a more potent Mcl-1 inhibitor, we sought to extend our molecules to occupy the entire BH3 binding interface. This was achieved using a fragment-based approach guided by structure-based design. Our efforts rapidly led to novel, potent Mcl-1 inhibitors that access additional pockets in the BH3 peptide binding groove. Three-dimensional structures of these new lead compounds when bound to Mcl-1 were extremely useful for designing inhibitors with better binding affinity and improved physicochemical properties.

RESULTS

Identification of Fragments that Bind to Additional Sites in the Mcl-1 BH3 Pocket

In order to guide the design of analogs that could bind to the P3 and P4 sites, we conducted a fragment-based screen of 13,824 molecules while the primary P2 site of Mcl-1 was saturated with compound **1**. The $^{1}H/^{15}N$ HSQC spectrum of compound **1** (K_i= 55 nM) bound to Mcl-1 served as the control spectrum from which any additional perturbations caused by fragment binding in other parts of the BH3-peptide binding groove could be detected.

Seven compounds **2-8** were identified that bind with millimolar affinities to Mcl-1 in the presence of **1**, (Figure 1). Hit **8** was the most potent fragment from this screen (K_d = 1.5 mM). All of the fragments bind to the same site based on the similar chemical shift perturbations that were observed. Although, these fragment hits only bind weakly to Mcl-1, a significant gain in affinity is anticipated by linking to compounds that bind to the P2 site[30].

Fragment Linker Design

Based on the chemical shift perturbations observed upon the addition of the fragment hits, we hypothesized that these molecules were binding to the hydrophobic pocket P4 occupied by the H4 residue of BH3-peptides[27]. In order to reach the P4 site, we explored the possibility of replacing the carboxylic acid of compound **1** with an acylsulfonamide, which would provide a synthetic handle for fragment linking while retaining the acidic functionality important for the interaction with R263. The methyl acylsulfonamide **9** was prepared, and it exhibited a 4-fold decrease in binding affinity when compared to the

parent acid (**1**). To explain this decrease in affinity, the co-crystal structure of **9** bound to Mcl-1 was obtained (Figure 2).

As shown in Figure 2, the methyl group of the acylsulfonamide of compound **9** points into the groove towards the P4 pocket. The acylsulfonamide group of **9** is next to R263 and maintains critical charged-charged interactions[13]. One of the sulfonyl oxygens is within H-bonding distance to the indole NH, which may increase the conformational stability of the functional group when bound. The addition of the sulfonamide functional group of **9** causes the molecule to tilt more than 2 Å away from the indole core position of **1** (Figure 2C), which could explain the loss of binding affinity. Despite this loss in affinity, the acylsulfonamide **9** has the advantage of providing a synthetic handle that could be used to link to the P4 fragment hits.

To design flexible linkers between the P4 fragments and a P2 pocket binder, we used the ternary structures of compound **10**, and two of our fragment hits **2** and **8** (Figure 3). These two ternary structures reveal that fragments **2** and **8** bind to the P4 site and are close to the methyl group of the acylsulfonamide. By superimposing the Mcl-1 BH3-peptide onto the structures (Figure 3C), it can be seen that both fragments occupy the P4 site. The fluorinated side-chain of our tightest binding fragment (**8**) fits into the P4 pocket and mimics the buried methyl group of the valine residue of the Mcl-1 BH3 peptide (Figure 3B). The spacing observed in these structures suggest that a flexible linker of three or four atoms could be used to link together compounds that bind in the Mcl-1 P2 pocket with fragments that bind to the P4 site.

Optimization of the Fragment Linker

Based on the two ternary structures, compounds with linkers containing two to four atoms were designed, synthesized, and tested utilizing two different prototypical fragments. A simple phenyl substituent was chosen to mimic the planar aromatic fragment hits and a cyclohexyl moiety to mimic the other fragments (Table 1). Starting from the methyl acylsulfonamide **11**, with a binding affinity of 655 nM, a 2-fold affinity gain was observed when a phenyl fragment was added using either a two-atom (**12**) or three-atom (**13**) linker. The addition of the cyclohexyl group with the three-atom linker as in compound **14** resulted in the greatest increase in binding affinity. However, extending the linker by one methylene unit (**15**) or incorporating a basic amine (**16**) caused a ten-fold decrease in potency from **14**. Changing the amide connection to a sulfonamide also reduced the binding affinity by a factor of two. These results suggest that a three-atom linker was preferred, in agreement with the X-ray structures (Figure 3). To separate the binding contribution of the cyclohexyl in the P4 site from the contributions of the flexible linker, we made compound **18**. This compound exhibited a 6-fold reduction in affinity by replacing the cyclohexyl of **14** with a methyl group suggesting that most of the added affinity of compound **14** comes from binding of the fragment unit into the P4 pocket. Finally, incorporation of a chlorine atom at the six position of the indole core resulted in an increase in binding affinity, as expected based on our previously described SAR[13]. From these initial studies, we demonstrated that we could link a P2 and P4 binder, increase the affinity and overcome the potency loss inherent in replacing the carboxylic acid with an acylsulfonamide.

Before further optimizing our compounds, we obtained an X-ray crystal structure of the linked compound **20**, an analog of **19**, containing a 1-naphthyl lower P2 pocket

binder. Alignment of the new crystal structure with the previously attained ternary structure (Figure 3A) shows a near perfect superposition (Figure 4) of the linked compound and the separate P2 and P4 binders. The cyclohexyl ring sits directly atop fragment **2**, reaffirming P4 as a hotspot with the potential for being utilized to gain an increase in binding affinity to Mcl-1. The linker spans a distance of 3.7 Å, almost identical to the spacing of 3.6 Å obtained from the ternary structure (Figure 3A). Most importantly, the binding conformation of the linked acylsulfonamide is now almost identical to the binding pose adopted for compound **10**, with only a slight rotation of the acylsulfonamide methyl.

Guided by the two ternary and linked compound co-crystal structures, we tested analogs of our fragment hits **2-7** (Table 2). When compared to compound **14** (K_i = 118 nM), incorporation of indole or benzofuran moieties (**21-25**) produced no improvement in binding affinity, regardless of the point of attachment. In an effort to combine the spatial characteristics of the indole and cyclohexyl fragments, a chiral indoline moiety was incorporated. Compound **26** containing a 2-(*S*)-indoline had better binding affinity to Mcl-1 than other fused bicyclic derivatives. Installation of the chlorine in the 6-position further improved the binding affinity. The 2-(*R*)- indoline enantiomer **28** exhibited the lowest K_i within the series (28 nM) with a 2-fold improvement compared to the benchmark cyclohexyl analog **19**. These results suggest that a non-planar geometry at the linking position is preferred.

Directly attaching pyrrole fragments **5** and **6** as exemplified in compounds **29** and **30** provided similar affinities as the cyclohexyl group of **14**. Removal of the pyrrole N1 substitution resulted in a significant reduction in inhibitory activity against Mcl-1 as

shown in compound **31**. However, this loss in affinity was fully recovered by capping the pyrrole NH with the methyl group (**32**), which resulted in a lower K_i than the analogs **14**, **29** and **30**. These results suggest that an H-bond donor at P4 is not beneficial, and aromatic N1 substitutions of fragment hits **5** and **6** are unnecessary for binding. Both compounds **33** and **34**, which contain a furan as the P4 unit, were also potent Mcl-1 inhibitors, and the 2-furanyl attachment was preferred at this site over the 1-position.

Substitutions based on analogs of the tightest binding fragment **8** were also tested. Initial linking of the 2-(1*H*-pyrazol-3-yl)phenol moiety in **35** increased binding affinity by a factor of two over the simple methyl-acylsulfonamide **11**. Reducing the fragment to a phenyl ring in compound **13** had little effect on affinity which suggests that the 5-6 linked aromatic scaffold of hit **8** may not be essential for binding at the P4 site. This is consistent with the co-crystal structure where the pyrazol of **8** is positioned outside of the pocket. To mimic the fluorinated side chain of fragment **8**, we tested simple fluorinated phenyl analogs **36**-**38**. These analogs showed a two to four-fold enhancement in affinity over the parent **13** (K_i = 430 nM) with the *meta*-fluoro isomer **37** being the most potent. Attempts to extend the fluorine substituents further into the P4 hydrophobic pocket produced trifluoromethyl derivatives **39**-**41**. These compounds also improved the affinity for Mcl-1 compared to **13** while showing a different positional preference for the substitution. Unlike fluorine, substitution of the phenyl with a CF_3 at the *ortho*-position (**39**, K_i = 18 nM) is four to six times more potent than the *meta*- (**40**) and *para*-isomers (**41**), respectively. These results suggest that introducing a fluorine atom at the correct location in the P4 pocket can enhance affinity, and that the per-fluorinated ethyl group of fragment **8** is likely the main contributor to its binding at this site.

To test this hypothesis, we explored the effect of adding small aliphatic groups at the P4 site. Compound **42**, containing a methyl P4 moiety, was used as the benchmark to further investigate this SAR. Adding a trifluoromethyl in **43** showed only a marginal improvement in binding affinity. However, extension of the carbon chain by an ethyl (**44**) or *iso*-propyl (**45**) group resulted in a two to three fold enhanced affinity for Mcl-1. The inclusion of extended branched alkyl groups (**46**, **47**) was found to significantly increase the binding affinity. These SAR trends can be rationalized by a close examination of the ternary structures of fragment **2** and **8** and the linked compound **20** (Figure 5), in which the sp3-hybridized C4 cyclohexyl methylene of **20** aligns with the planar indole and pyrazole units of the fragments. These data suggested that removal of the C4 methylene would likely improve shape complementarity with the pocket. The concept was applied in the design of compound **46**, which showed a 4-fold improvement in affinity when compared with the cyclohexyl analog **19**. Finally, the most potent inhibitor **47** (K_i = 10 nM) in this series was obtained by extending the branching point of the P4 moiety of **45** by one methylene, which led to an overall 7-fold affinity enhancement. This substituent and its position is similar to that observed for the valine in the Mcl-1 BH3 peptide[28].

Our structural data (Figure 5) suggested that the flexible ethylene portion of the linker could be replaced by a 5-6 membered ring to connect the P4 moiety to the acylsulfonamide. This modification would reduce the number of rotatable bonds and could improve permeability and other drug like properties of the molecules[31]. Various rigid linker groups were tested (compounds **49-52)** and it was found that incorporation of cyclic aromatic groups resulted in higher affinities for Mcl-1 than the analogous methyl

acylsulfonamides **9** and **11** (Table 3). To rationalize the improved affinity of the cyclic linker units, a co-crystal structure of compound **49** bound to Mcl-1 was obtained (Figure 6). The structure shows that the phenyl linker points to the P4 pocket, while the acylsulfonamide group maintains the critical charged-charged interaction with R263 similar to the methyl analog **9** (Figure 6A). Unlike the methyl acylsulfonamide **9**, the conformation of the P2 binding unit in **49** adopts the higher affinity pose that was observed in our original acid analog **1** (Figure 6B). These observed conformational changes likely explain the improvement in affinity for **49** and **50**. All of the Ar groups listed in Table 3 gave similar affinities.

To further improve the binding affinity of the acylsulfonamide series, we investigated the effect of substitutions on the indole core. In previous work, it was shown that substitutions at the 7-position resulted in enhanced binding affinities for 2-indole acids[14]. To investigate if this was also true for our phenyl acylsulfonamides, we added both 5 and 6-membered heteroaryl groups to the 7-position of the indole. As shown in Table 4, the unsubstituted pyridine-3-yl group in **53** caused a marginal increase in affinity while analogs **54** and **55** containing a methyl group next to the indole linking position exhibited 10- and 26-fold enhanced potency against Mcl-1 relative to **49**. These results strongly suggested that substitutions on the 7-aryl group could enhance binding by adopting a conformation where the methyl group points towards the P3 site much like the earlier indole acids[14]. This hypothesis was supported by compound **56** where an orthogonal conformation of the 3,5-di-Me-1*H*-pyrazole group to the indole core would be favored to relieve the steric congestion exerted by the two methyl groups. We next tested if 6-Cl analogs would give a further synergistic boost in affinity[13]. Compounds **57**-**59**

were prepared and when tested all of the 6-Cl analogs exhibited binding affinities below the level able to be accurately determined in our Fluorescence Polarization Anisotropy (FPA) assay conditions based on the concentration of Mcl-1 and the affinity of our peptide based FITC-Bak probe.

For compounds **56**-**59** (Table 4), with affinities higher than could be determined in our original assay, we measured their K_i's in the presence of 1% Fetal Bovine Serum (FBS). This approach assesses the effect of serum protein binding on the inhibitory activity of the ligand to Mcl-1[32], and affinities measured under the condition can be a good predictor of activity in cellular assays. This approach has been used in other studies of Mcl-1[14] and other Bcl-2[33] family members as a predictor of efficacy in cell assays. Using this assay for ranking, we found that the 6-Cl group further enhanced the series, with compound **59** having the highest potency in the presence of 1% FBS.

The binding mode of **49** (Figure 6) suggested that substitutions on the 4-position of a phenyl or 5-position of a furan could be used to reach the P4 pocket. Because the amide group of N260 sits along the path to P4, we decided to test polar linking groups. Compounds **60**-**61**, having a furan-5-carboxylic acid moiety, were prepared to test the hypothesis. We found that their binding affinities were still well below the level able to be accurately determined in our FPA assay. To understand their binding mode, a structure of **60** complexed to Mcl-1 was determined (Figure 7). As expected, the di-methyl pyrazole adopts a nearly orthogonal conformation to the indole core, and the 6-Cl is in the P2 pocket adjacent to helix 4. In addition, the newly introduced carboxylic acid is positioned in the groove within H-bonding distance to the amide NH of N260 explaining the observed enhancement in the binding affinity. It can also be seen in the

structure that the NH of the pyrazole points out of the binding pocket, and thus methylation of the pyrazole in **61** did not affect Mcl-1 affinity. These results suggest that an additional group could be introduced at the NH of the pyrazole to improve the drug-like characteristics of the inhibitors or to generate a small molecule probe for biochemical assays without reducing binding to Mcl-1. Unfortunately, Both **60** and **61** do not show measurable permeability in the PAMPA assay, which is likely due to having two acidic functional groups.

This information was used to make a new high affinity small molecule probe **62** by linking a fluorescein label (2-(6-hydroxy-3-oxo-3H-xanthen-9-yl)benzoic acid) to the NH of the pyrazole of **60** through a flexible spacer unit. Indeed, this probe exhibited a K_d of 0.46 nM in FPA based equilibrium binding assay as a function of Mcl-1 concentration (Figure 8a). This probe is 37-fold more potent than the Bak peptide based probe (K_d = 17 nM) used in our first assay. The corresponding parent **60** and **61** were tested in competitive binding experiments to test their ability to displace the probe **62** from Mcl-1 and showed K_i's of 0.36 and 0.78 nM (Figure 8b), respectively, that were in good agreement with K_d of the labeled probe. The new probe has excellent sensitivity, aqueous solubility, and chemical stability for a FPA binding assay and was the easiest to implement in our workflow and was thus used to determine the affinities for all subsequent potent Mcl-1 inhibitors.

Compounds **63**-**75** shown in Table 5 represent Mcl-1 inhibitors that contain all of the features that we found to increase affinity in our exploratory SAR including an optimized indole P2 unit and incorporation of P4 fragment with a rigid aromatic linker. The first set of compounds **63**-**69** was constructed by connecting beneficial P4 binders

identified from the earlier studies, to the 3 position of the phenyl linker with an amide group. The attachment position and spacing are consistent with the Mcl-1 co-crystal structure of compound **49** (Figure 6B). These compounds exhibited potent inhibitory activities beyond the detection limit of the Bak peptide probe, and had K_i's in the range of 42-92 nM in the presence of 1% FBS. When binding affinities were measured using the new small molecule probe **62**, we found that the SAR trends found on less elaborated scaffolds were mostly conserved when combined in the compounds of Table 5. The increase in affinity from the parent core in **50** to the 7-tri-methyl-pyrazole analog **59** was further compounded by addition of P4 binders. The high affinity of compound **66** (K_i = 2.9 nM) showed 6-fold improvement in potency when compared to the parent **59**, and the 3-furanyl group in **35** was also one of the optimal P4 substituents in the flexible linker series.

Amide analogs of **61**, compounds **70** and **71**, were designed based on the Mcl-1 co-crystal structure with **60** (Figure 7). P4 site fragments were connected using a reverse amide linker to preserve the beneficial H-bond found between the terminal acetate of **60** and N260. Indeed, compound **70** bound to Mcl-1 with high affinity (K_i = 2.4 nM) to confirm the effectiveness of the new linker unit. Compound **71** containing the 4-pyridyl P4 moiety showed 3.5-fold weaker Mcl-1 affinity than the phenyl analog **70**, however in the [12]fact, compound **71** maintained the highest affinity among all examples in Table 5 in 1% FBS suggesting that serum protein binding for the series could be minimized by the 4-pyridyl moiety.

Our earlier SAR also suggested a pyridyl linker could be as effective as a phenyl group (compound **49** vs. **51**) and has better pharmaceutical properties. Therefore,

compounds **72**-**75** were prepared to test the feasibility of a 4-pyridyl linker by connecting P4 groups through an amine bridge. These compounds were also found to be very potent Mcl-1 inhibitors with compounds **73** and **75** exhibiting K_i's of 1 nM.

These results suggest that the rigid aromatic linker effectively delivers a P4 binder with enhanced conformational stability while maintaining a high affinity conformation at the P2 site. Indeed, compounds **63**-**75** have substantial affinity improvements (up to 17 fold in the presented examples) compared to the parent phenyl acylsulphonamide **59**. These compounds still have high protein binding and poor permeability (e.g. compound 70, 72-75 have Pampa permeability $< 3.0\ 10^{-6}$ cm/s) and these two factors likely contribute to their high micromolar EC_{50} in cell viability studies (data not shown). Although these compounds are potent Mcl-1 inhibitors, earlier work on Bcl-2 family inhibitors[12] including Mcl-1[15] indicate that picomolar inhibitors with low protein binding is necessary for robust cell activity. In the supplementary material, we show evidence of activity in a pull down assay in cell lysates. This experiment does not depend on cell permeability and protein binding (Figure S1 Supplementary material).

Selectivity profile over Bcl-xL

The selectivity of compounds for Mcl-1 over Bcl-xL was tested using the anti-apoptotic protein Bcl-xL in the Bak FPA assay (Table 5). As can be seen in Table 5, all of the tested compounds exhibited only weak affinity for Bcl-xL with a greater than 500-fold window in affinity. As found in our previous studies, structural modifications on the series that enhance the affinity for Mcl-1 had relatively little effect on improving binding to Bcl-xL. As a result, the compounds became more selective against Bcl-xL as they

became more potent for Mcl-1. A selective Mcl-1 inhibitor is preferred because it could be more easily co-dosed with selective inhibitors of other family members to induce apoptosis[34] and to manage potential liabilities[11].

Synthesis

All acylsulfonamides were prepared according to methods outlined in Scheme 1-4. The synthetic route employed for the preparation of the indole-carboxylic acid cores was reported previously[13, 16]. Experimental details are described in the supporting information. In Scheme 1, the simplest acyl sulfonamides were synthesized using the general coupling reaction condition from either commercially available sulfonamides or sulfonamides prepared from the parent sulfonyl chloride by treatment with ammonia. The more elaborate linked acylsulfonamides were prepared through sulfonamide derivatization followed by general coupling from the commercially available carboxylic acids or acid chlorides when possible in a one-pot procedure. Linked acylsulfonamides with simple aliphatic R-groups were prepared utilizing the linear synthesis method due to the difficulty of monitoring the formation of the sulfonamide intermediates. 7-Ar-indole-2-phenyl-acylsulfonamide derivatives **53**-**59** shown in Scheme 2 were prepared from the corresponding ethyl 7-Br-indole-2-carboxylate using Suzuki coupling protocols followed by the general coupling reaction with phenylsulfonamide. Scheme 3 describes synthesis of the fluorescein probe **62**. The 3,5-dimethyl-pyrazol-1-yl acetate was installed on the indole core then the Boc protected di-aminohexane spacing unit was coupled. Subsequent saponification liberated 2-indole carboxylic acid, which was converted to the furanyl-acylsulfonamide **81**. Sequence of deprotection reactions yield the zwitterionic intermediate **82**. The fluorescein label was then connected *via* an amide linkage to give

isomeric mixture of probe **62**. Finally, Scheme 4 summarizes syntheses of fully elaborated Mcl-1 inhibitors shown in Table 5.

CONCLUSION

Here we demonstrated a fragment-based strategy to improve the affinity of Mcl-1 inhibitors by accessing additional pockets on Mcl-1. We showed that by accessing the P4 pocket we could substantially improve affinity. These studies resulted in compounds that exhibited a binding affinity increase of a hundred fold from the initial methyl acysulfonamide lead **9** and clearly demonstrates that affinity gains can be achieved by filling additional pockets in the BH3 groove. Structural studies were important to guide and then verify the correct position of the fragments in the final linked compound. Initial benchmark studies using a flexible linker were used to identify minimal P4 binding units. These data were exploited in the next stage when we used rigid scaffolds as linkers to reduce the number of rotatable bonds in the final compounds. The structural and SAR data obtained on these linked ligands can now be used to design more potent Mcl-1 inhibitors with better pharmaceutical properties.

EXPERIMENTAL SECTION

Chemistry

General. All NMR spectra were recorded at room temperature on a 400 MHz AMX Bruker spectrometer. ^{1}H chemical shifts are reported in δ values in ppm downfield with the deuterated solvent as the internal standard. Data are reported as follows: chemical shift, multiplicity (s = singlet, d = doublet, t = triplet, q = quartet, br = broad, m =

multiplet), integration, coupling constant (Hz). Low resolution mass spectra were obtained on an Agilent 1200 series 6140 mass spectrometer with electrospray ionization. All samples were of ≥95% purity as analyzed by LC−UV/vis-MS. Analytical HPLC was performed on an Agilent 1200 series with UV detection at 214 and 254 nm along with ELSD detection. LC/MS parameters were as follows: Phenomenex-C18 Kinetex column, 50 x 2.1 mm, 2 min gradient, 5% (0.1% TFA/MeCN) / 95% (0.1% TFA/ H_2O) to 100% (0.1% TFA/MeCN). Preparative purification was performed on a Gilson HPLC (Phenomenex-C18, 100 x 30 mm, 10 min gradient, 5→95% MeCN/H_2O with 0.1% TFA) or by automated flash column chromatography (Isco, Inc. 100sg Combiflash). Solvents for extraction, washing, and chromatography were HPLC grade. All reagents were purchased from chemical suppliers and used without purification.

Protein expression and purification. A codon-optimized gene sequence encoding residues 172-327 of human Mcl-1 (Uniprot: *Q07820*) was purchased (Genscript) and cloned into a Gateway entry vector (pDONR-221, Invitrogen) using the protocols provided. This construct was further sub-cloned into an expression vector (pDEST-HisMBP) containing a maltose binding protein (MBP) tag for increased solubility, a tobacco etch virus (TEV) protease recognition site for tag-removal and an N-terminal His-tag to facilitate purification. The integrity of all plasmids was checked by sequencing. Soluble Mcl-1 protein was expressed in *Escherichia coli* BL21 CodonPlus (DE3) RIL (Stratagene) using ampicillin and chloramphenicol for selection.

In brief, a colony from a fresh transformation plate was picked to inoculate 100 mL of LB medium (37°C). The overnight culture was used to start a 10 L fermentation

(BioFlo 415, New Brunswick Scientific) grown at 37°C. When the cell density corresponded to OD_{600}=2, the temperature was lowered to 20°C. After one hour, protein expression was induced with 0.5 mM IPTG. Cells were harvested after 16 h by centrifugation. Pellets were frozen and re-dissolved in lysis buffer (20 mM TRIS pH 7.5, 300 mM NaCl, 20 mM imidazole, 5 mM BME), approximately 100 mL / 10 g pellet, before the cells were broken by homogenization (APV-2000, APV). Prior to application to an affinity column (140 mL, ProBond, Invitrogen), lysate was cleared by centrifugation (18,000 rpm) and filtration (0.44 µm). Bound protein was washed on the column and then eluted by a gradient (20 mM TRIS pH 7.5, 300 mM NaCl, 500 mM imidazole, 5 mM BME). To enhance TEV protease cleavage, samples were buffer exchanged (50 mM TRIS pH 7.5, 100 mM NaCl, 5 mM BME) on three serially connected columns (HiPrep 26/10 Desalting, GE Healthcare). TEV protease was added to a molar ratio of 1:10 (TEV:Mcl-1) and incubated at room temperature until cleavage was complete. After adding 20 mM imidazole to the samples, they were passed over a subtractive second nickel-column (120 mL, Ni-NTA Superflow, Qiagen) to remove the MBP-tag, non-cleaved protein, and TEV protease. To achieve highly pure samples (e.g. for crystal screening), a supplementary step of size-exclusion chromatography (HiLoad 26/60, Superdex 75, GE Healthcare) was implemented. The running buffer also acted as the Mcl-1 storage and crystallography buffer (20 mM HEPES pH 6.8, 50 mM NaCl, 3 mM DTT, 0.01% NaN_3). Purifications were done at 4°C, and concentration steps were performed in stirred ultrafiltration cells (Amicon, Millipore).

To improve protein sample quality and to increase crystal diffraction, protein mutants were created by site-directed mutagenesis (QuikChange, Agilent Technologies).

Primers for a C-terminal deletion (Δ5) were designed using their online tool and ordered from Eurofins MWG Operon. Mutations were made on the entry vector above, analyzed by in-house sequencing, and subsequently transferred into the pDEST-HisMBP expression vector. Mutant proteins were purified in the same way as wild-type (WT) proteins.

Protein crystallization, data collection and structure refinement. Fresh batches of Mcl-1 proteins, WT and Δ5, were concentrated to 600 μM (10.7 mg/mL) and 1 mM (17.4 mg/mL), respectively, and screened for crystallization conditions with a 1.2x excess of ligand. Crystals were obtained by mixing 1 μL protein with 1 μL reservoir solution (25-30% PEG 3350, 0.1 M Bis-TRIS pH 6.5, 0.2 M $MgCl_2$) as a hanging drop at 4°C or 18°C. Crystals appeared within the first week and were flash frozen in liquid nitrogen after cryoprotection using 10-20% glycol.

Data were collected on the Life Sciences Collaborative Access Team (LS-CAT) 21-ID-D beamline at the Advanced Photon Source (APS), Argonne National Laboratory. Indexing, integration and scaling was performed with HKL2000[35]. Using a previously determined ligand-bound structure (PDB: 4HW2), phasing was done by molecular replacement with Phaser[36] as implemented in CCP4[37]. Refinement of the structural models were performed with Phenix and Refmac, and included rounds of manual model building in COOT[38]. Figures were prepared in PyMOL[39].

Competition Assays. A fluorescein isothiocyanate (FITC)-labeled BH3 peptide derived from Bak (FITC-Bak-BH3; FITC-AHx-GQVGRQLAIIGDDINR-NH2) was purchased from GenScript and used without further purification. For our most potent compounds a new high affinity probe, **62** was used. FPA measurements were carried out in 384-well,

black, flat-bottom plates (Greiner Bio-One) using the BioTek Cytation 3 plate reader. All assays were conducted in assay buffer containing 20 mM TRIS pH 7.5, 50 mM NaCl, 3 mM DTT, and 5% final DMSO concentration. To measure displacement of the FITC-Bak-BH3 peptide from Bcl-2 family members, 10 nM FITC-Bak-BH3 peptide was incubated with either 15 nM Mcl-1 or 4 nM Bcl-xL. To measure displacement of **62** from Mcl-1, 0.4 nM of **62**, was incubated with 0.5 nM Mcl-1. For IC_{50} determination, compounds were diluted in DMSO in a 10-point, 3-fold serial dilution scheme, added to assay plates, and incubated for 1.5 h at room temperature. The change in anisotropy was measured and used to calculate an IC_{50} (inhibitor concentration at which 50% of bound probe is displaced) by fitting the anisotropy data using XLFit (IDBS) to a four parameter dose-response (variable slope) equation. This was converted into a binding dissociation constant (K_i) according to the formula[40]:

$$K_i = [I]_{50}/([L]_{50}/K_d + [P]_0/K_d + 1)$$

where $[I]_{50}$ is the concentration of the free inhibitor at 50% inhibition, $[L]_{50}$ is the concentration of the free labeled ligand at 50% inhibition, $[P]_0$ is the concentration of the free protein at 0% inhibition and K_d^{pep} represents the dissociation constant of the FITC-labeled peptide probe. Compounds were evaluated using replicate measurement, in duplicate; K_i values shown are the average of duplicate values.

FPA saturation binding assays for 62. A fluorescein labeled small molecule probe **62** was titrated with the Mcl-1 protein. FPA measurements were conducted under the same condition as described above. To measure association of the probe to Mcl-1, 0.4 nM **62** was incubated with varying concentration of the Mcl-1 protein prepared by a 14-point, 2-fold serial dilution with the top concentration equaling 100 nM.

ASSOCIATED CONTENT

Supporting Information

X-ray crystallography statistics, Dose-dependent blocking of Mcl-1 pulldown in cell lysates. Synthesis details. This material is available free of charge via the Internet at http://pubs.acs.org.

Accession Codes

Atom coordinates and structure factors for Mcl-1/ligand complexes have been deposited at the Protein Data Bank ID codes: 5FC4, 5FDO, 5FDR

AUTHOR INFORMATION

Corresponding Author

*Phone: +1 (615) 322 6303. Fax: +1 (615) 875 3236. E-mail:stephen.fesik@vanderbilt.edu.

Present Addresses

! AbbVie Pharmaceuticals, North Chicago, IL

^ Bayer HealthCare, Berlin 13353, Germany

+ The institute of cancer research, Sutton, UK

Notes

The authors declare no competing financial interest.

ACKNOWLEDGMENT

The authors thank co-workers at the High-Throughput Screening Core facility of Vanderbilt University, TN, for compound management and providing the instrumentation

to perform the binding assay. This research was supported by the U.S. National Institutes of Health, NIH Director's Pioneer Award DP1OD006933/DP1CA174419 to S.W.F., The NCI Experimental Therapeutics (NExT) Program BOA29XS129TO22 under the Leidos Biomed Prime Contract No. HHSN261200800001E, and a career development award to S.W.F. from a NCI SPORE grant in breast cancer (Grant P50CA098131) to C. L. Arteaga. The Biomolecular NMR Facility at Vanderbilt University is supported in part by a NIH SIG Grant 1S-10RR025677-01 and Vanderbilt University matching funds. Use of the Advanced Photon Source was supported by the U.S. Department of Energy, Office of Science, Office of Basic Energy Sciences, under Contract No. DE-AC02-06CH11357.

ABBREVIATIONS

Mcl-1, myeloid cell leukemia 1; Bcl-2, B-cell lymphoma 2; Bcl-xL, B-cell lymphoma extra large; BH3, Bcl-2 homology domain 3; Bax, Bcl-2-associated X protein; Bak, Bcl-2 homologous antagonist killer; FITC, fluorescein isothiocyanate; FPA, fluorescence polarization anisotropy.

REFERENCES

1. Reed, J. C. Bcl-2 and the regulation of programmed cell death. *J. Cell. Biol.* **1994**, *124*, 1-6.

2. Danial, N. N.; Korsmeyer, S. J. Cell death: critical control points. *Cell* **2004**, *116*, 205-219.

3. Hanahan, D.; Weinberg, R. A. The hallmarks of cancer. *Cell* **2000**, *100*, 57-70.

4. Hanahan, D.; Weinberg, R. A. Hallmarks of cancer: the next generation. *Cell* **2011**, *144*, 646-674.

5. Kitanaka, C.; Namiki, T.; Noguchi, K.; Mochizuki, T.; Kagaya, S.; Chi, S.; Hayashi, A.; Asai, A.; Tsujimoto, Y.; Kuchino, Y. Caspase-dependent apoptosis of COS-7 cells induced by Bax overexpression: differential effects of Bcl-2 and Bcl-xL on Bax-induced caspase activation and apoptosis. *Oncogene* **1997**, *15*, 1763-1772.

6. Adams, J. M.; Cory, S. The Bcl-2 apoptotic switch in cancer development and therapy. *Oncogene* **2007**, *26*, 1324-1337.

7. Igney, F. H.; Krammer, P. H. Death and anti-death: tumour resistance to apoptosis. *Nat. Rev. Cancer* **2002**, *2*, 277-288.

8. Ghobrial, I. M.; Witzig, T. E.; Adjei, A. A. Targeting apoptosis pathways in cancer therapy. *CA Cancer J. Clin.* **2005**, *55*, 178-194.

9. Delbridge, A. R.; Strasser, A. The BCL-2 protein family, BH3-mimetics and cancer therapy. *Cell Death Differ.* **2015**, *22*, 1071-1080.

10. Tse, C.; Shoemaker, A. R.; Adickes, J.; Anderson, M. G.; Chen, J.; Jin, S.; Johnson, E. F.; Marsh, K. C.; Mitten, M. J.; Nimmer, P.; Roberts, L.; Tahir, S. K.; Xiao, Y.; Yang,

X.; Zhang, H.; Fesik, S.; Rosenberg, S. H.; Elmore, S. W. ABT-263: a potent and orally bioavailable Bcl-2 family inhibitor. *Cancer Res.* **2008**, *68*, 3421-3428.

11. Kaefer, A.; Yang, J.; Noertersheuser, P.; Mensing, S.; Humerickhouse, R.; Awni, W.; Xiong, H. Mechanism-based pharmacokinetic/pharmacodynamic meta-analysis of navitoclax (ABT-263) induced thrombocytopenia. *Cancer Chemother. Pharmacol.* **2014**, *74*, 593-602.

12. Souers, A. J.; Leverson, J. D.; Boghaert, E. R.; Ackler, S. L.; Catron, N. D.; Chen, J.; Dayton, B. D.; Ding, H.; Enschede, S. H.; Fairbrother, W. J.; Huang, D. C.; Hymowitz, S. G.; Jin, S.; Khaw, S. L.; Kovar, P. J.; Lam, L. T.; Lee, J.; Maecker, H. L.; Marsh, K. C.; Mason, K. D.; Mitten, M. J.; Nimmer, P. M.; Oleksijew, A.; Park, C. H.; Park, C. M.; Phillips, D. C.; Roberts, A. W.; Sampath, D.; Seymour, J. F.; Smith, M. L.; Sullivan, G. M.; Tahir, S. K.; Tse, C.; Wendt, M. D.; Xiao, Y.; Xue, J. C.; Zhang, H.; Humerickhouse, R. A.; Rosenberg, S. H.; Elmore, S. W. ABT-199, a potent and selective BCL-2 inhibitor, achieves antitumor activity while sparing platelets. *Nat. Med.* **2013**, *19*, 202-208.

13. Friberg, A.; Vigil, D.; Zhao, B.; Daniels, R. N.; Burke, J. P.; Garcia-Barrantes, P. M.; Camper, D.; Chauder, B. A.; Lee, T.; Olejniczak, E. T.; Fesik, S. W. Discovery of potent myeloid cell leukemia 1 (Mcl-1) inhibitors using fragment-based methods and structure-based design. *J. Med. Chem.* **2013**, *56*, 15-30.

14. Bruncko, M.; Wang, L.; Sheppard, G. S.; Phillips, D. C.; Tahir, S. K.; Xue, J.; Erickson, S.; Fidanze, S.; Fry, E.; Hasvold, L.; Jenkins, G. J.; Jin, S.; Judge, R. A.; Kovar, P. J.; Madar, D.; Nimmer, P.; Park, C.; Petros, A. M.; Rosenberg, S. H.; Smith, M. L.; Song, X.; Sun, C.; Tao, Z. F.; Wang, X.; Xiao, Y.; Zhang, H.; Tse, C.; Leverson, J.

D.; Elmore, S. W.; Souers, A. J. Structure-guided design of a series of MCL-1 inhibitors with high affinity and selectivity. *J. Med. Chem.* **2015**, *58*, 2180-2194.

15. Leverson, J. D.; Zhang, H.; Chen, J.; Tahir, S. K.; Phillips, D. C.; Xue, J.; Nimmer, P.; Jin, S.; Smith, M.; Xiao, Y.; Kovar, P.; Tanaka, A.; Bruncko, M.; Sheppard, G. S.; Wang, L.; Gierke, S.; Kategaya, L.; Anderson, D. J.; Wong, C.; Eastham-Anderson, J.; Ludlam, M. J.; Sampath, D.; Fairbrother, W. J.; Wertz, I.; Rosenberg, S. H.; Tse, C.; Elmore, S. W.; Souers, A. J. Potent and selective small-molecule MCL-1 inhibitors demonstrate on-target cancer cell killing activity as single agents and in combination with ABT-263 (navitoclax). *Cell Death Dis.* **2015**, *6*, e1590.

16. Burke, J. P.; Bian, Z.; Shaw, S.; Zhao, B.; Goodwin, C. M.; Belmar, J.; Browning, C. F.; Vigil, D.; Friberg, A.; Camper, D. V.; Rossanese, O. W.; Lee, T.; Olejniczak, E. T.; Fesik, S. W. Discovery of tricyclic indoles that potently inhibit Mcl-1 using fragment-based methods and structure-based design. *J. Med. Chem.* **2015**, *58*, 3794-3805.

17. Abulwerdi, F. A.; Liao, C.; Mady, A. S.; Gavin, J.; Shen, C.; Cierpicki, T.; Stuckey, J. A.; Showalter, H. D.; Nikolovska-Coleska, Z. 3-Substituted-N-(4-hydroxynaphthalen-1-yl)arylsulfonamides as a novel class of selective Mcl-1 inhibitors: structure-based design, synthesis, SAR, and biological evaluation. *J. Med. Chem.* **2014**, *57*, 4111-4133.

18. Petros, A. M.; Swann, S. L.; Song, D.; Swinger, K.; Park, C.; Zhang, H.; Wendt, M. D.; Kunzer, A. R.; Souers, A. J.; Sun, C. Fragment-based discovery of potent inhibitors of the anti-apoptotic MCL-1 protein. *Bioorg. Med. Chem. Lett.* **2014**, *24*, 1484-1488.

19. van Delft, M. F.; Wei, A. H.; Mason, K. D.; Vandenberg, C. J.; Chen, L.; Czabotar, P. E.; Willis, S. N.; Scott, C. L.; Day, C. L.; Cory, S.; Adams, J. M.; Roberts, A. W.;

Huang, D. C. The BH3 mimetic ABT-737 targets selective Bcl-2 proteins and efficiently induces apoptosis via Bak/Bax if Mcl-1 is neutralized. *Cancer Cell* **2006**, *10*, 389-399.

20. Lin, X.; Morgan-Lappe, S.; Huang, X.; Li, L.; Zakula, D. M.; Vernetti, L. A.; Fesik, S. W.; Shen, Y. 'Seed' analysis of off-target siRNAs reveals an essential role of Mcl-1 in resistance to the small-molecule Bcl-2/Bcl-XL inhibitor ABT-737. *Oncogene* **2007**, *26*, 3972-3979.

21. Wertz, I. E.; Kusam, S.; Lam, C.; Okamoto, T.; Sandoval, W.; Anderson, D. J.; Helgason, E.; Ernst, J. A.; Eby, M.; Liu, J.; Belmont, L. D.; Kaminker, J. S.; O'Rourke, K. M.; Pujara, K.; Kohli, P. B.; Johnson, A. R.; Chiu, M. L.; Lill, J. R.; Jackson, P. K.; Fairbrother, W. J.; Seshagiri, S.; Ludlam, M. J.; Leong, K. G.; Dueber, E. C.; Maecker, H.; Huang, D. C.; Dixit, V. M. Sensitivity to antitubulin chemotherapeutics is regulated by MCL1 and FBW7. *Nature* **2011**, *471*, 110-114.

22. Wei, S. H.; Dong, K.; Lin, F.; Wang, X.; Li, B.; Shen, J. J.; Zhang, Q.; Wang, R.; Zhang, H. Z. Inducing apoptosis and enhancing chemosensitivity to gemcitabine via RNA interference targeting Mcl-1 gene in pancreatic carcinoma cell. *Cancer Chemother. Pharmacol.* **2008**, *62*, 1055-1064.

23. Beroukhim, R.; Mermel, C. H.; Porter, D.; Wei, G.; Raychaudhuri, S.; Donovan, J.; Barretina, J.; Boehm, J. S.; Dobson, J.; Urashima, M.; Mc Henry, K. T.; Pinchback, R. M.; Ligon, A. H.; Cho, Y. J.; Haery, L.; Greulich, H.; Reich, M.; Winckler, W.; Lawrence, M. S.; Weir, B. A.; Tanaka, K. E.; Chiang, D. Y.; Bass, A. J.; Loo, A.; Hoffman, C.; Prensner, J.; Liefeld, T.; Gao, Q.; Yecies, D.; Signoretti, S.; Maher, E.; Kaye, F. J.; Sasaki, H.; Tepper, J. E.; Fletcher, J. A.; Tabernero, J.; Baselga, J.; Tsao, M. S.; Demichelis, F.; Rubin, M. A.; Janne, P. A.; Daly, M. J.; Nucera, C.; Levine, R. L.;

Ebert, B. L.; Gabriel, S.; Rustgi, A. K.; Antonescu, C. R.; Ladanyi, M.; Letai, A.; Garraway, L. A.; Loda, M.; Beer, D. G.; True, L. D.; Okamoto, A.; Pomeroy, S. L.; Singer, S.; Golub, T. R.; Lander, E. S.; Getz, G.; Sellers, W. R.; Meyerson, M. The landscape of somatic copy-number alteration across human cancers. *Nature* **2010**, *463*, 899-905.

24. Placzek, W. J.; Wei, J.; Kitada, S.; Zhai, D.; Reed, J. C.; Pellecchia, M. A survey of the anti-apoptotic Bcl-2 subfamily expression in cancer types provides a platform to predict the efficacy of Bcl-2 antagonists in cancer therapy. Cell Death Dis 2010, 1, e40.

25. Arkin, M. R.; Wells, J. A. Small-molecule inhibitors of protein-protein interactions: progressing towards the dream. *Nat. Rev. Drug Discov.* **2004**, *3*, 301-17.

26. Petros, A. M.; Olejniczak, E. T.; Fesik, S. W. Structural biology of the Bcl-2 family of proteins. *Biochim. Biophys. Acta.* **2004**, *1644*, 83-94.

27. Czabotar, P. E.; Lessene, G.; Strasser, A.; Adams, J. M. Control of apoptosis by the BCL-2 protein family: implications for physiology and therapy. *Nat. Rev. Mol. Cell Biol.* **2014**, *15*, 49-63.

28. Stewart, M. L.; Fire, E.; Keating, A. E.; Walensky, L. D. The MCL-1 BH3 helix is an exclusive MCL-1 inhibitor and apoptosis sensitizer. *Nat. Chem. Biol.* **2010**, *6*, 595-601.

29. Czabotar, P. E.; Lee, E. F.; van Delft, M. F.; Day, C. L.; Smith, B. J.; Huang, D. C.; Fairlie, W. D.; Hinds, M. G.; Colman, P. M. Structural insights into the degradation of Mcl-1 induced by BH3 domains. *Proc. Natl. Acad .Sci.* **2007**, *104*, 6217-6222.

30. Shuker, S. B.; Hajduk, P. J.; Meadows, R. P.; Fesik, S. W. Discovering high-affinity ligands for proteins: SAR by NMR. *Science* **1996**, *274*, 1531-1534.

31. Di, L.; Kerns, E. H. Profiling drug-like properties in discovery research. *Curr. Opin. Chem. Biol.* **2003**, *7*, 402-408.

32. Liu, X.; Wright, M.; Hop, C. E. Rational use of plasma protein and tissue binding data in drug design. *J. Med. Chem.* **2014**, *57*, 8238-8248.

33. Oltersdorf, T.; Elmore, S. W.; Shoemaker, A. R.; Armstrong, R. C.; Augeri, D. J.; Belli, B. A.; Bruncko, M.; Deckwerth, T. L.; Dinges, J.; Hajduk, P. J.; Joseph, M. K.; Kitada, S.; Korsmeyer, S. J.; Kunzer, A. R.; Letai, A.; Li, C.; Mitten, M. J.; Nettesheim, D. G.; Ng, S.; Nimmer, P. M.; O'Connor, J. M.; Oleksijew, A.; Petros, A. M.; Reed, J. C.; Shen, W.; Tahir, S. K.; Thompson, C. B.; Tomaselli, K. J.; Wang, B.; Wendt, M. D.; Zhang, H.; Fesik, S. W.; Rosenberg, S. H. An inhibitor of Bcl-2 family proteins induces regression of solid tumours. *Nature* **2005**, *435*, 677-681.

34. Goodwin, C. M.; Rossanese, O. W.; Olejniczak, E. T.; Fesik, S. W. Myeloid cell leukemia-1 is an important apoptotic survival factor in triple-negative breast cancer. *Cell Death Differ.* **2015**, *22*, 2098-2106.

35. Otwinowski, Z.; Minor, W. Processing of X-ray Diffraction Data Collected in Oscillation Mode. In Macromolecular Crystallography. Part A; Carter, C. W., Jr., Sweet, R. M., Eds.; Academic Press: San Diego, CA, 1997; Vol. *276*, pp 307–326.

36. McCoy, A. J.; Grosse-Kunstleve, R. W.; Adams, P. D.; Winn, M. D.; Storoni, L. C.; Read, R. J. Phaser crystallographic software. *J. Appl. Crystallogr.* **2007**, *40*, 658-674.

37. Collaborative Computational Project, N. The CCP4 suite: programs for protein crystallography. *Acta. Crystallogr. D. Biol. Crystallogr.* **1994**, *50*, 760-763.

38. Emsley, P.; Cowtan, K. Coot: model-building tools for molecular graphics. *Acta. Crystallogr. D. Biol. Crystallogr.* **2004**, *60*, 2126-2132.

39. The PyMOL Molecular Graphics System, version 1.5; Schrödinger, LLC: New York, **2010**.

40. Nikolovska-Coleska, Z.; Wang, R.; Fang, X.; Pan, H.; Tomita, Y.; Li, P.; Roller, P. P.; Krajewski, K.; Saito, N. G.; Stuckey, J. A.; Wang, S. Development and optimization of a binding assay for the XIAP BIR3 domain using fluorescence polarization. *Anal. Biochem.* **2004**, *332*, 261-273.

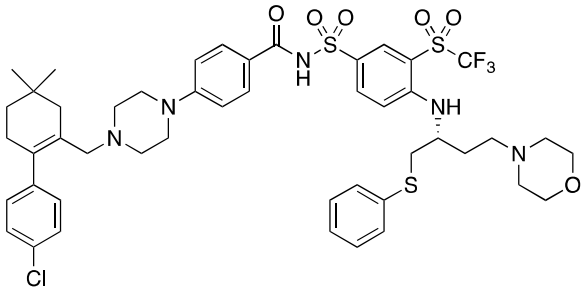

Navitoclax (ABT-263)

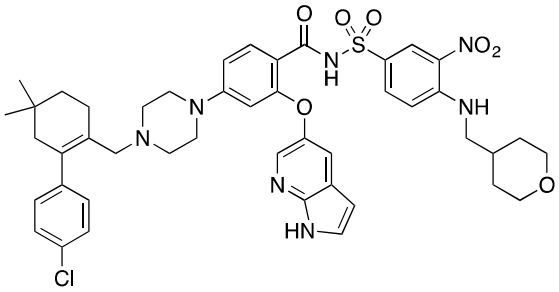

Venetoclax (ABT-199)

Figure 1. Fragment hits (2-8) identified by an NMR screen using compound **1** to block the initial binding pocket.

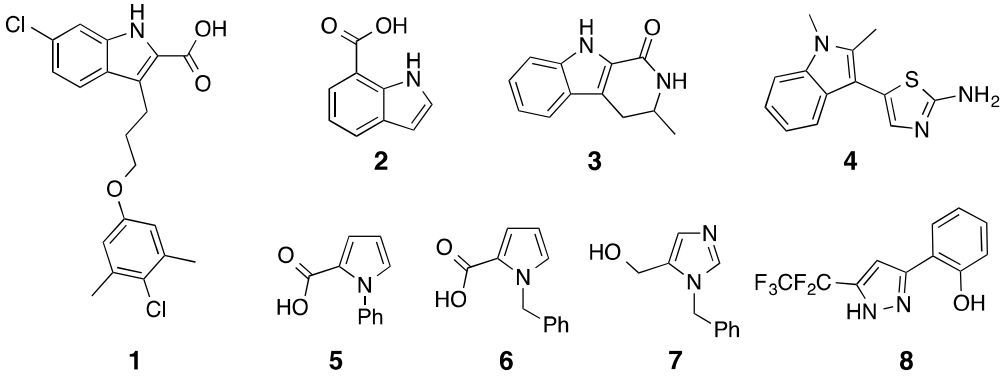

Figure 2: Overlay illustrating the different binding conformations of carboxylic acid **1** and the acylsulfonamide analog **9**. (A) Structure of **9** and its Mcl-1 inhibition constant. (B) Important polar contacts of **9** (B) **9** fills P2 and is adjacent to additional pockets of the BH3 binding groove.

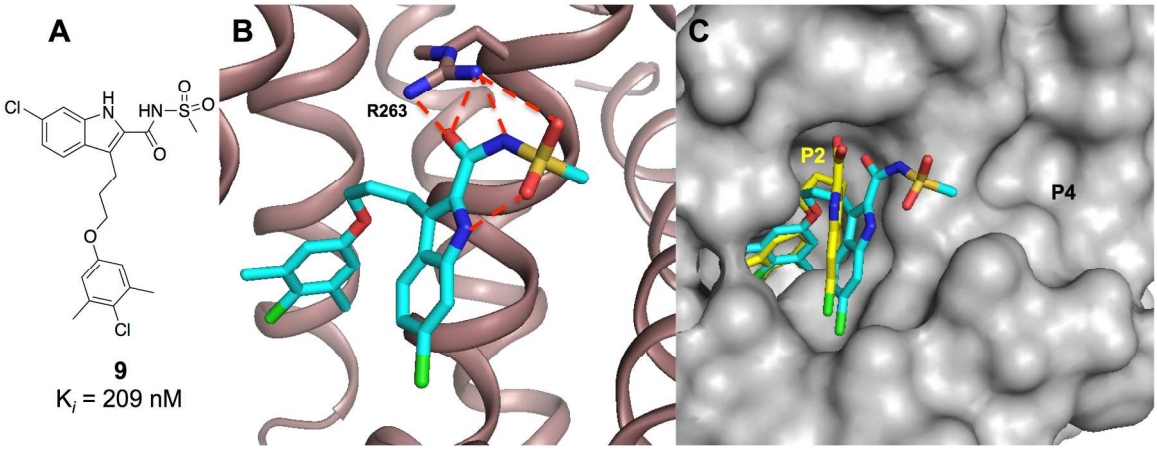

Figure 3: Ternary X-ray co-crystal structures (A) Fragment **2** bound to Mcl-1 in the presence of acylsulfonamide **10.** (B) Fragment **8** bound to Mcl-1 in the presence of acylsulfonamide **10**. (C) Superposition of 16-mer Mcl-1 BH3 peptide (ID: 4HW4) and the two fragment hits. (D) Structure of **10** and its Mcl-1 inhibition constant.

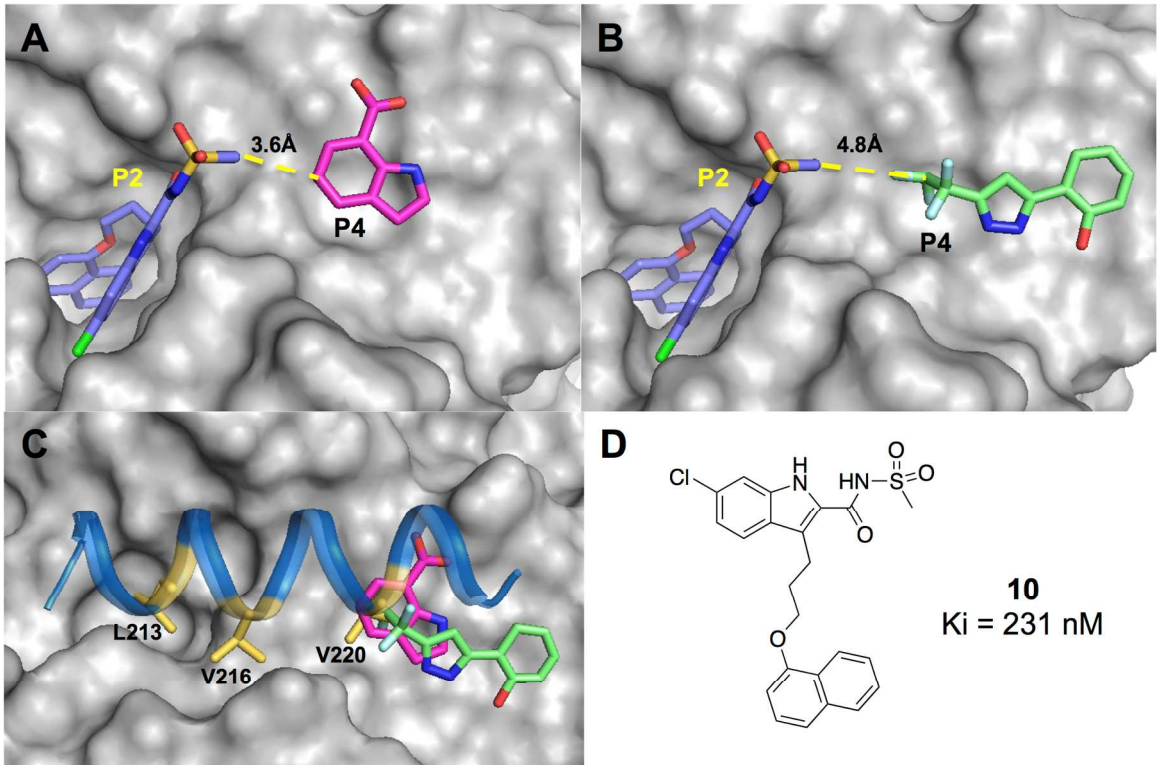

Figure 4: Overlay of linked compound **20** and a ternary X-ray structure of **10** and fragment **2**.

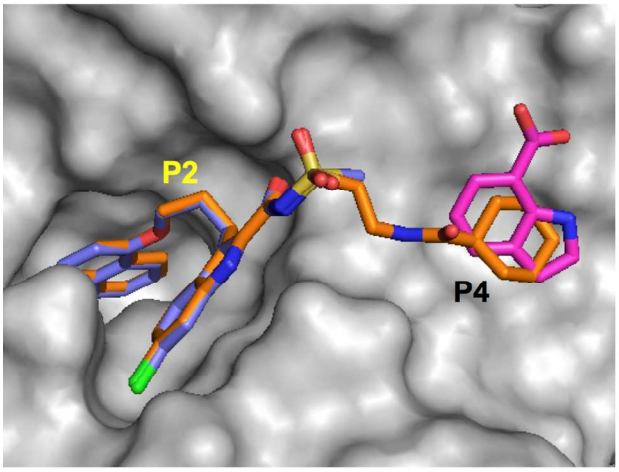

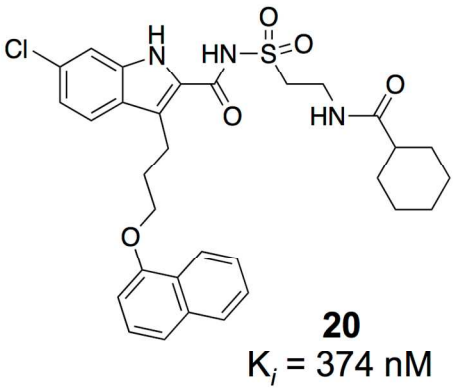

Figure 5: Overlay of the co-crystal structure of compound **20** and fragments **2** and **8** bound to Mcl-1.

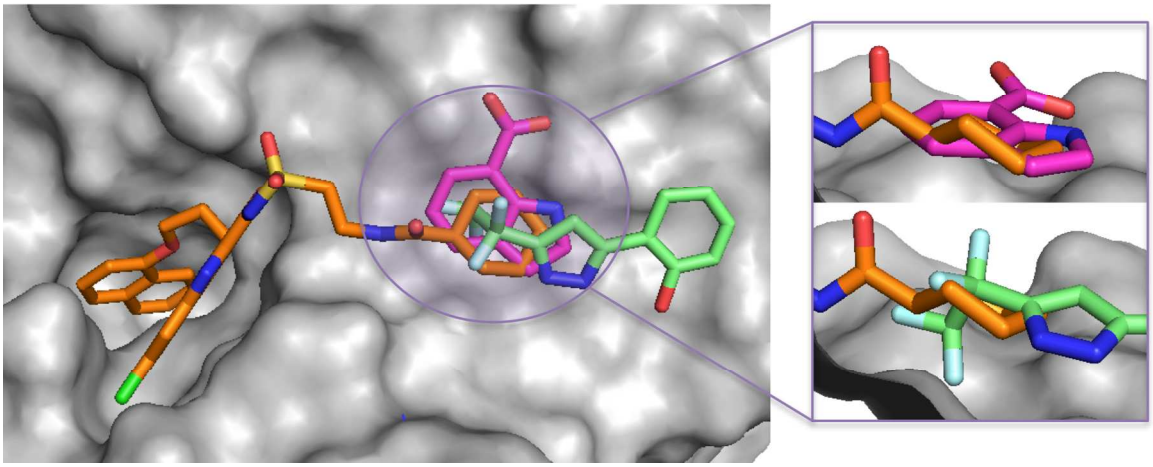

Figure 6. Mcl-1 co-crystal structure with compound **49** (A) polar contacts of **49** (B) **49** binds in the P2 pocket in a high affinity pose and is adjacent to additional pockets of the BH3 binding groove.

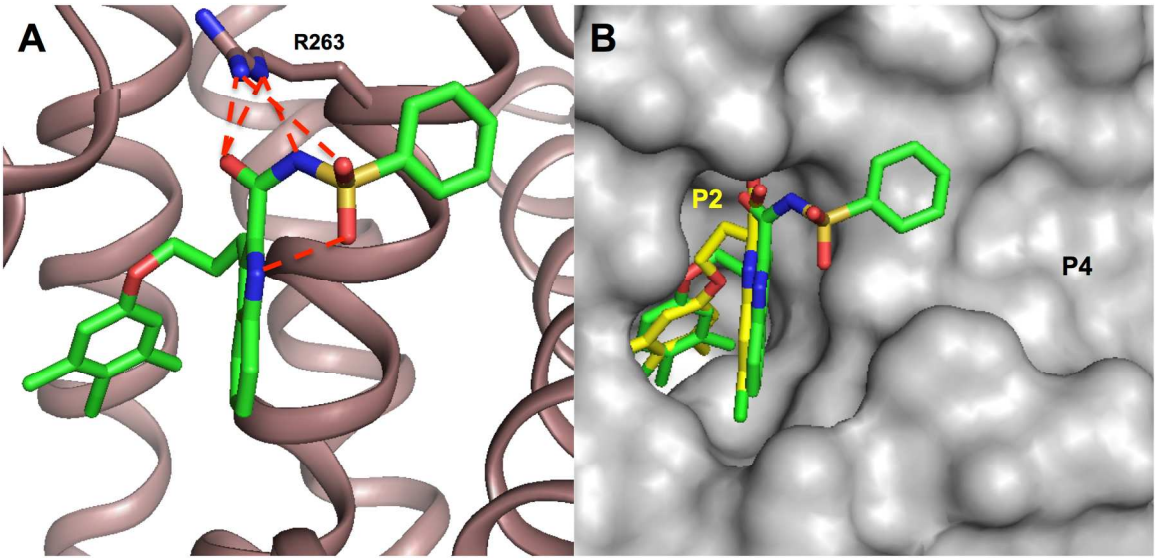

Figure 7. Development of a tight binding fluorescent Mcl-1 probe. (A) Compound **60** binds to the Mcl-1 BH3 groove and (B) polar contacts of **60** to R263 and N260.

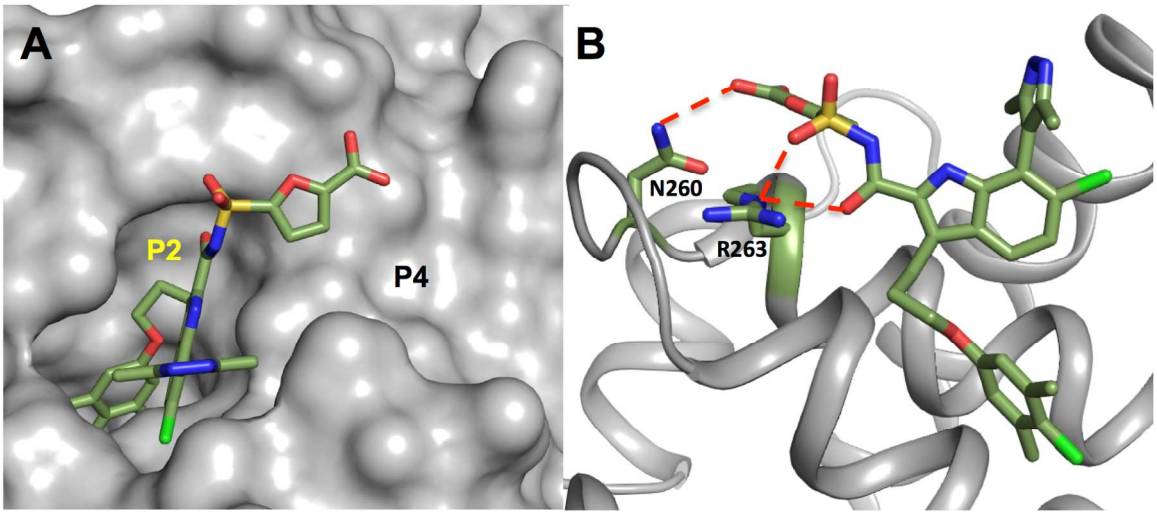

Figure 8. (A) Binding curve of the fluorescent small molecule probe **62** to Mcl-1. (B) Displacement of probe **62** from Mcl-1 by compounds **60** and **61**.

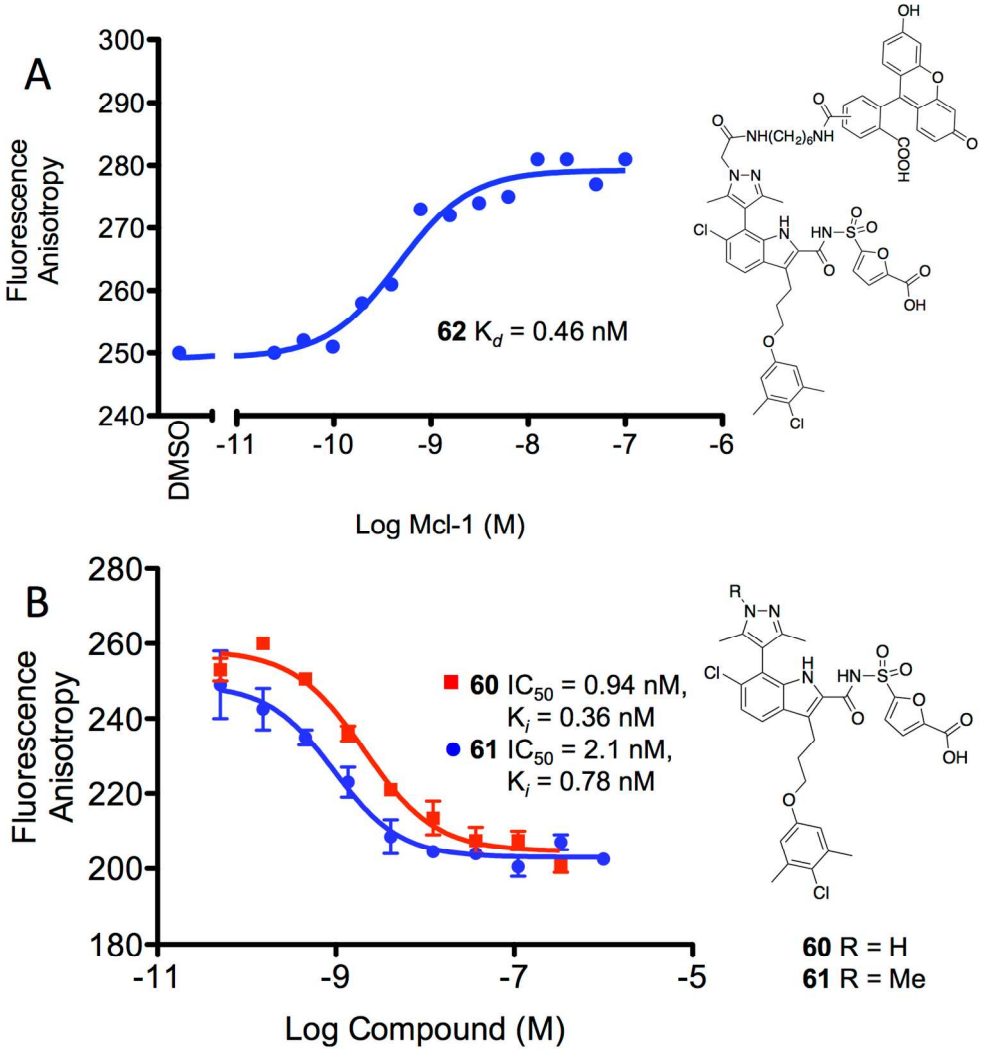

Table 1: Linker Optimization

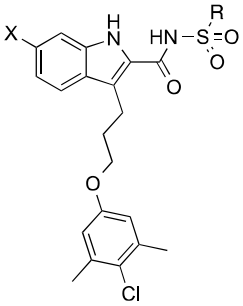

CM	X	R	K_i (nM)
11	H	Me	655
12	H	CH_2CH_2OPh	322
13	H	$CH_2CH_2NH(C{=}O)Ph$	430
14	H	$CH_2CH_2NH(C{=}O)Cy$	118
15	H	$CH_2CH_2NH(C{=}O)CH_2Cy$	1098
16	H	$CH_2CH_2CH_2NHCy$	1015
17	H	$CH_2CH_2NH(SO_2)Cy$	251
18	H	$CH_2CH_2NH(C{=}O)Me$	656
19	Cl	$CH_2CH_2NH(C{=}O)Cy$	55

Table 2: P4 Fragment Incorporation and Optimization

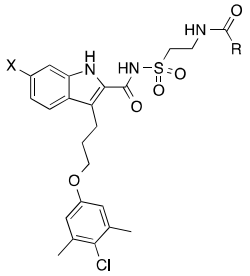

CM	R	X	Y	K_i (nM)
21		H		269
22		H		278
23		H		432
24		H		298
25		H		311
26		H		193
27		Cl		46
28	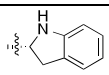	Cl		28
29		H	Ph	139
30		H	Bn	148
31		Cl	H	782
32		H	Me	90
33		Cl		53

34		Cl		19
35	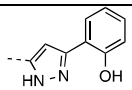	Cl		308
36	2-F-phenyl	H		336
37	3-F-phenyl	H		100
38	4-F-phenyl	H		117
39	2-CF_3-phenyl	Cl		18
40	3-CF_3-phenyl	Cl		79
41	4-CF_3-phenyl	Cl		119
42	Me	Cl		209
43	CF_3	Cl		116
44	Et	Cl		87
45	*i*-Pr	Cl		66
46	3-Pentyl	Cl		16
47	*i*-Bu	Cl		10

Table 3. Binding affinities of aromatic acylsulfonamides

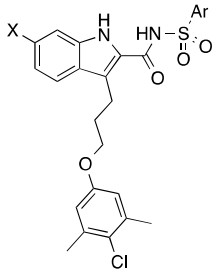

CM	Ar	X	K_i (nM)
49	Ph	H	361
50		Cl	91
51	4-pyridyl	H	335
52	1-furanyl	Cl	116

Table 4. Effect of 7-Ar group in binding affinity of phenyl 2-indole-acylsulfonamides

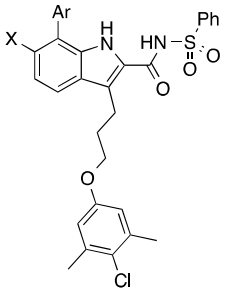

CM	Ar	X	K_i (nM) Bak	K_i (nM) 1% FBS	K_i (nM) 62
53	Pyridin-3-yl	H	202	n.d.	n.d.
54	4-Me-pyridin-3-yl	H	36	n.d.	n.d.
55	2-Me-pyridin-3-yl	H	14	n.d.	n.d.
56	3,5-di-Me-pyrazol-4-yl	H	<10	517	n.d.
57	2-Me-pyridin-3-yl	Cl	<10	146	18
58	3,5-di-Me-pyrazol-4-yl	Cl	<10	147	n.d.
59	1,3,5-tri-Me-pyrazol-4-yl	Cl	<10	64	17

n.d.= not determined

Table 5. Optimization of Mcl-1 binding affinity by incorporation of P4 binding moieties.

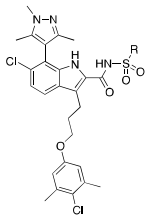

CM	R	K_i (nM) Bak	K_i (nM) 1% FBS	K_i (nM) 62	K_i (nM) Bcl-xL
63	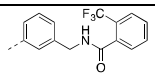	<10	80	5.0	4467
64	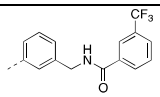	<10	78	7.0	12854
65	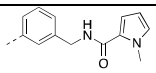	<10	91	10.0	>50000
66	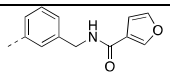	<10	69	2.9	1404
67	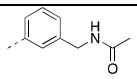	<10	42	11.1	9069
68	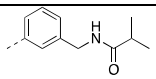	<10	54	16.0	>50000
69	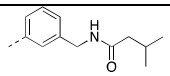	<10	92	5.6	1566
70	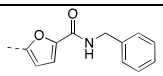	<10	84	2.4	>50000
71	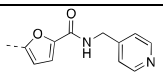	<10	20	8.5	>50000

72	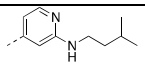	<10	179	5.6	4467
73	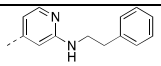	<10	78	1.2	1109
74	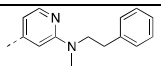	<10	226	2.5	943
75	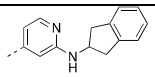	<10	61	1.0	997

n.d.= not determined

Scheme 1: Acylsulfonamide Synthesis

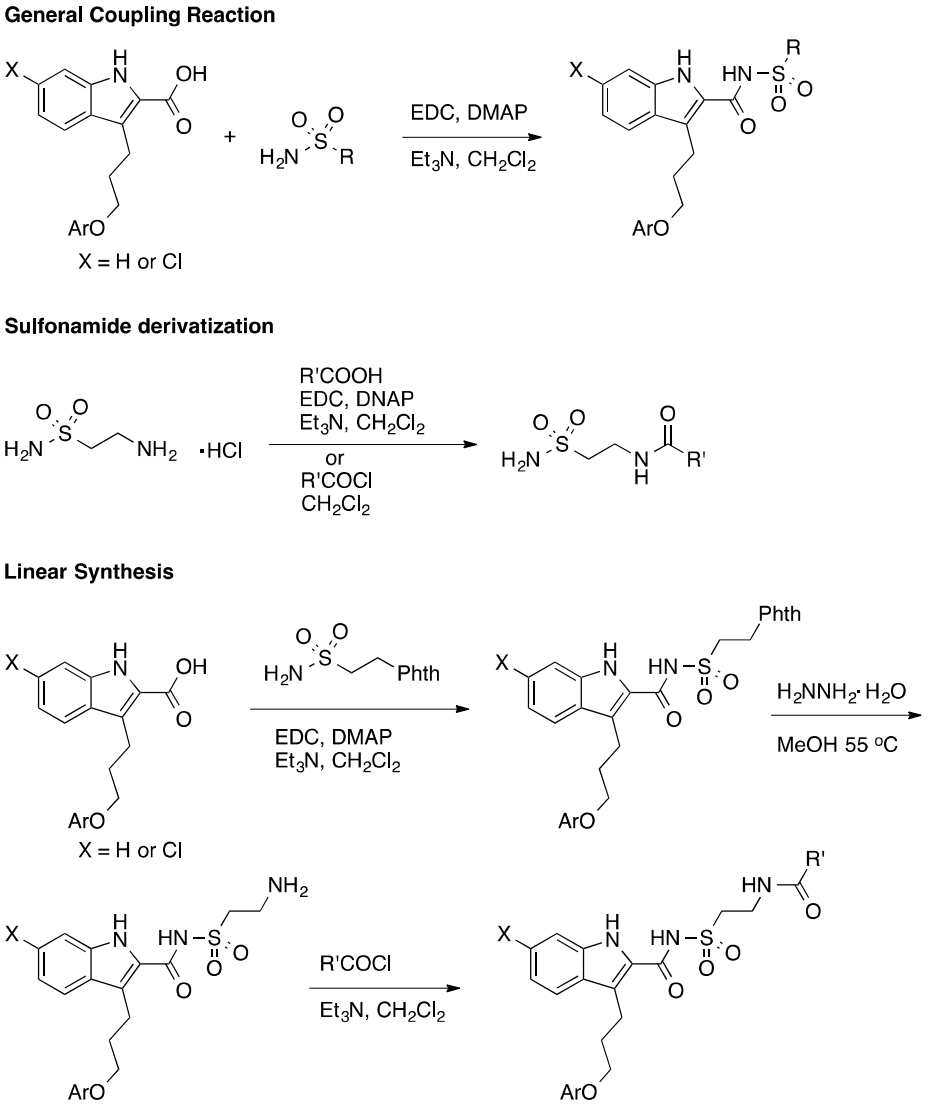

Scheme 2. Synthesis of 7-Ar-indole-2-phenyl-acylsulfonamide derivatives.

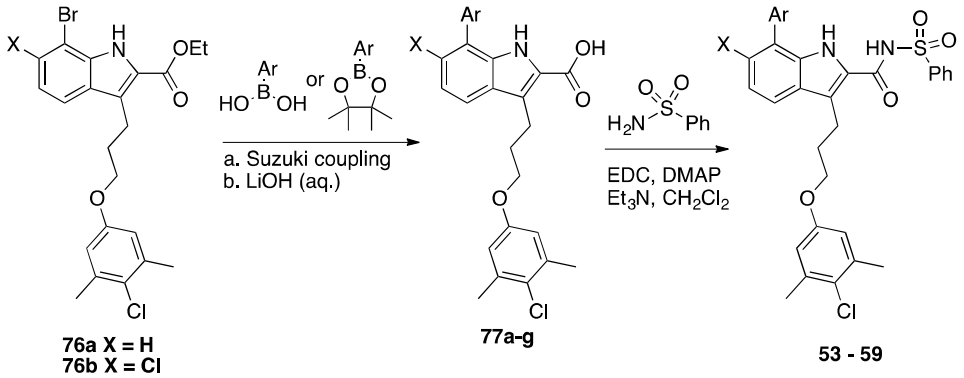

Scheme 3. Preparation of the fluorescein label small molecule probe **62**.

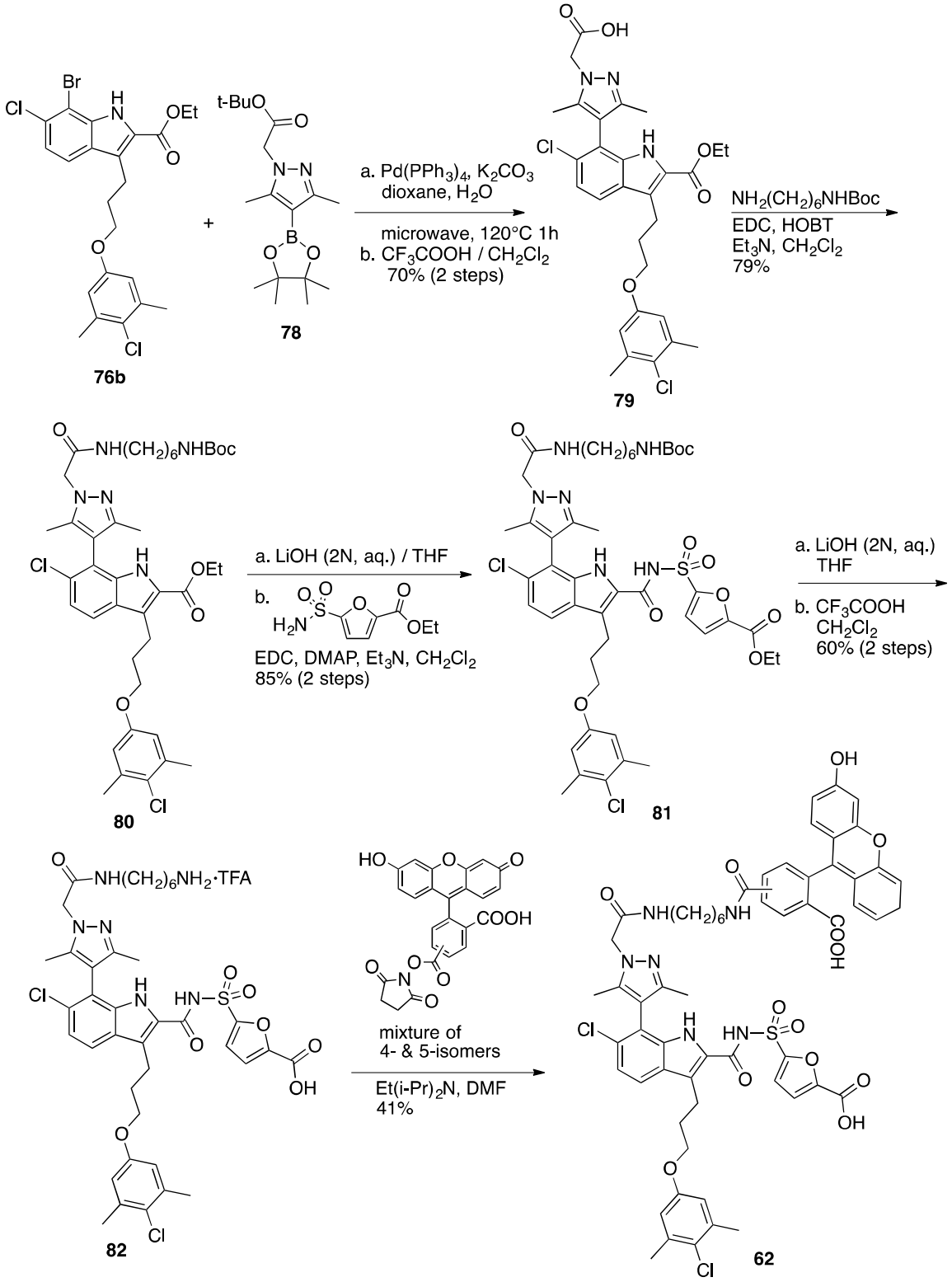

Scheme 4. Preparation of compounds 63-75.

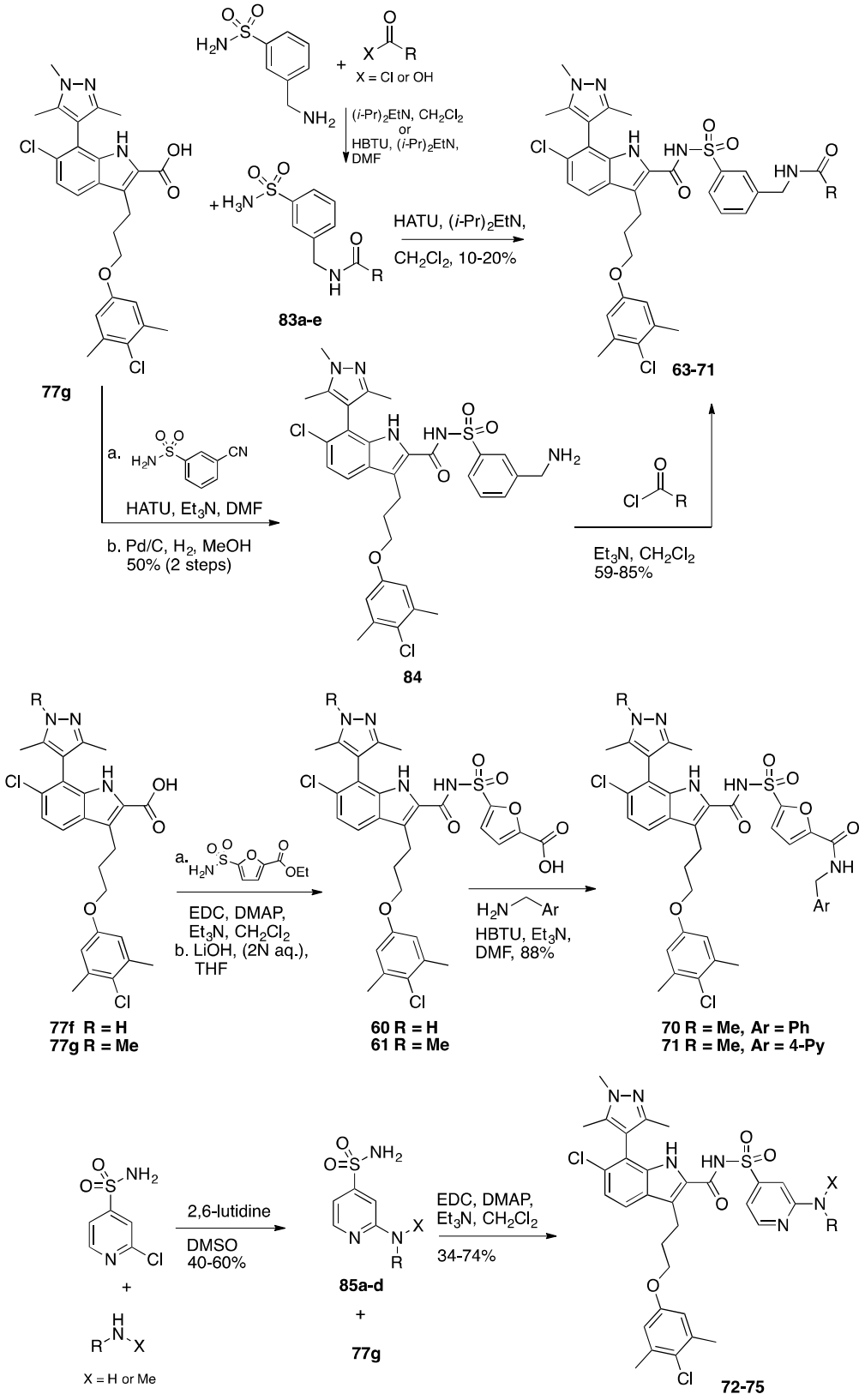

Table of Contents graphic.

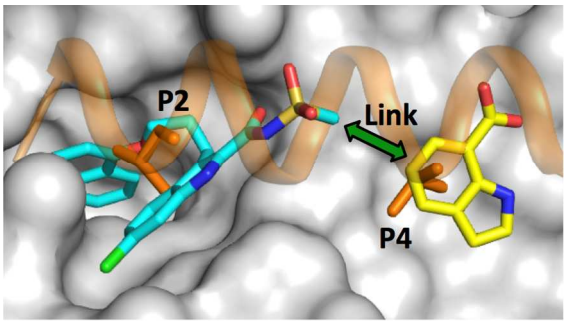

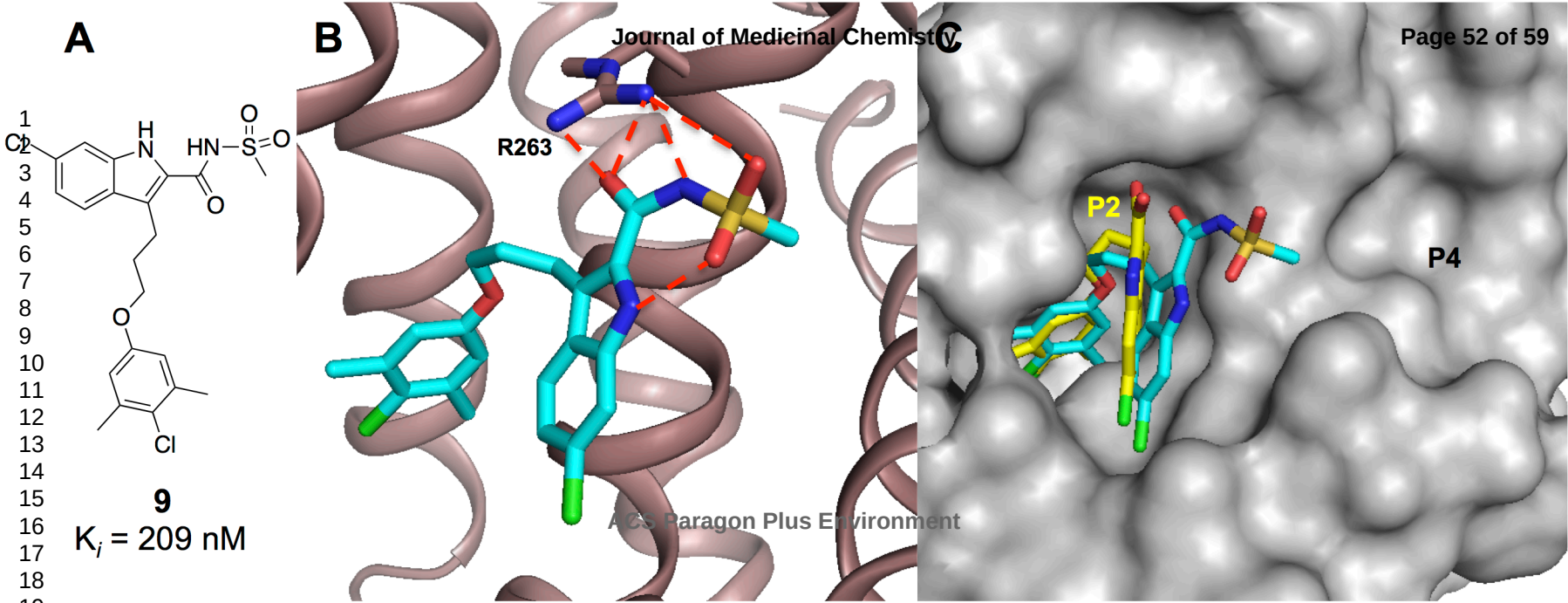

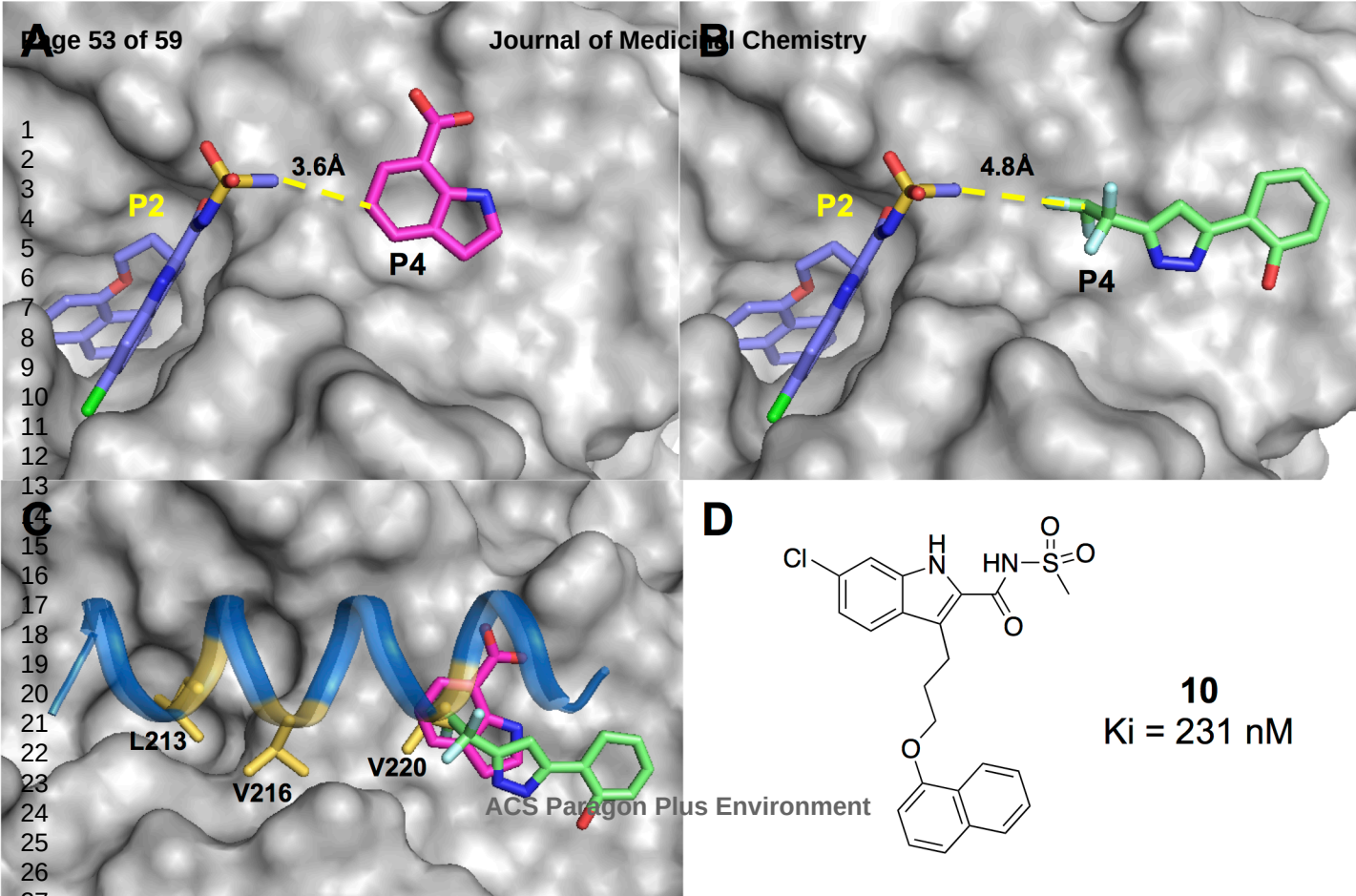

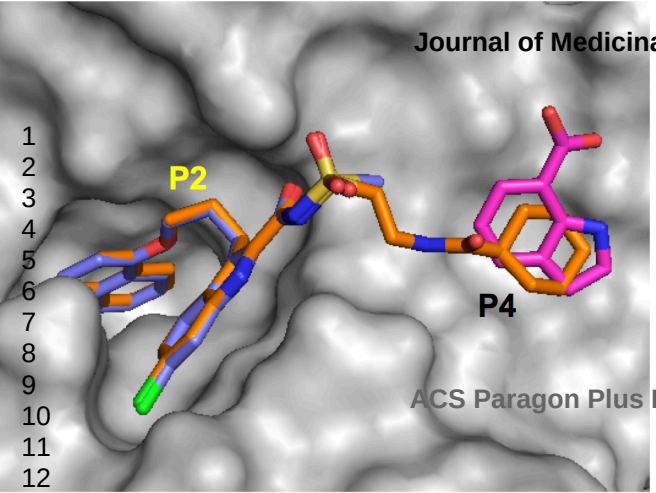

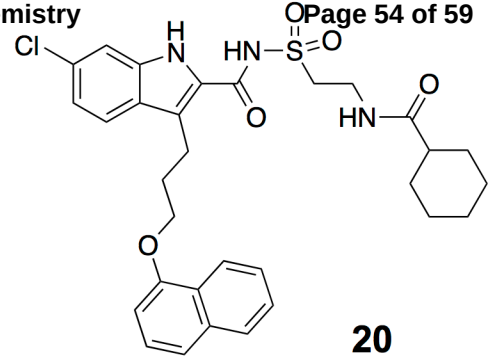

20

K_i = 374 nM

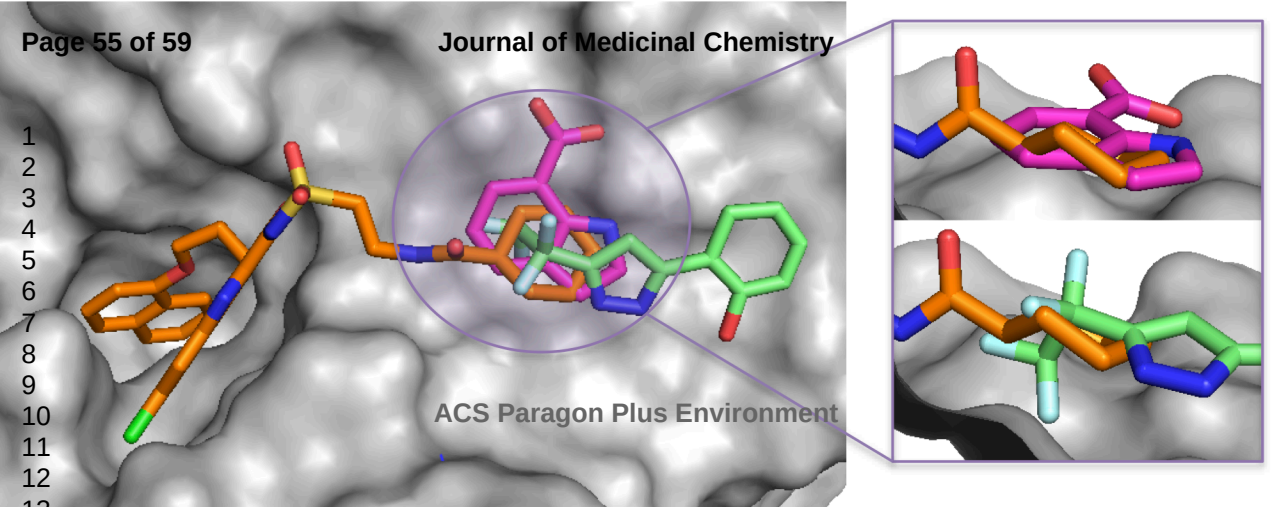
ACS Paragon Plus Environment

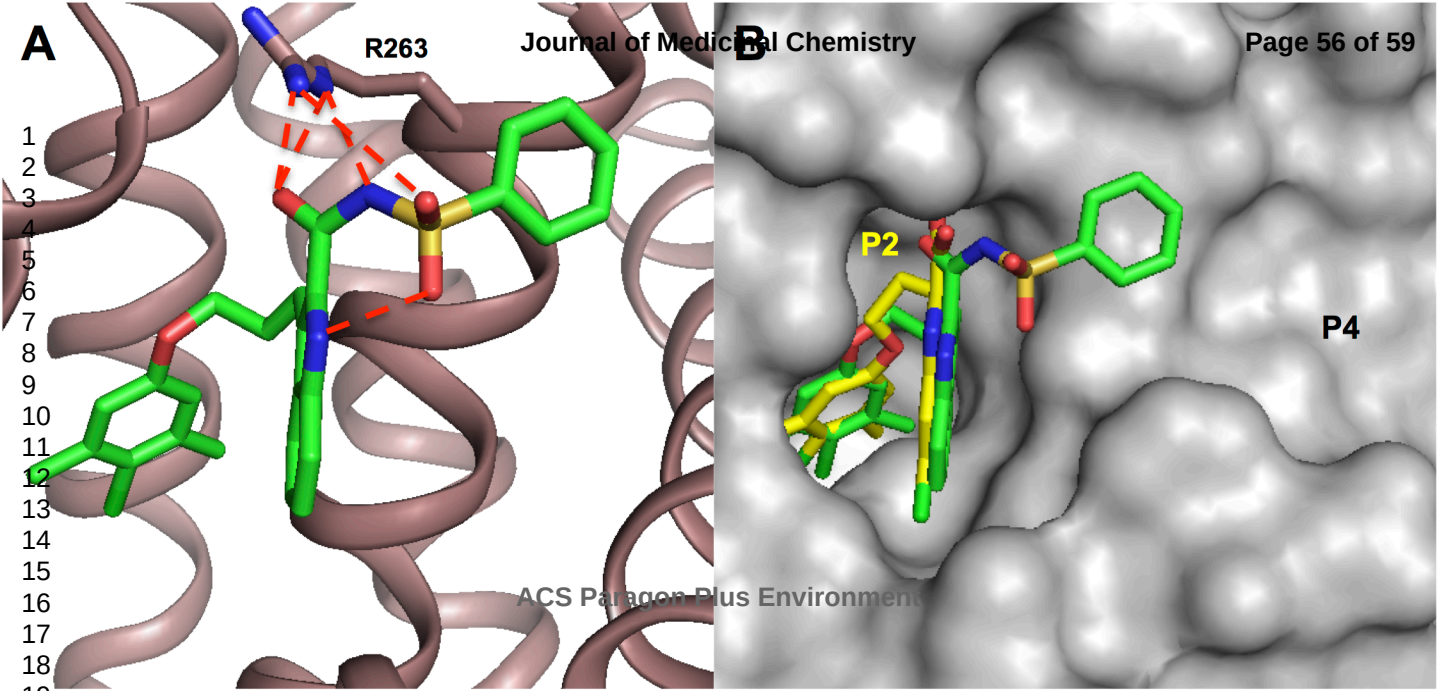

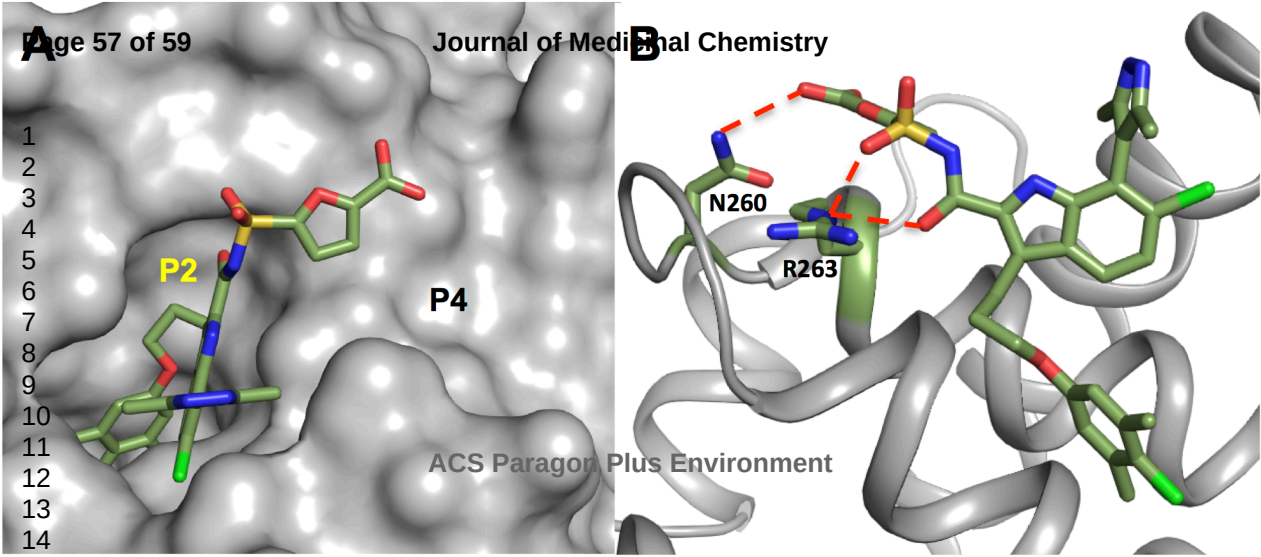

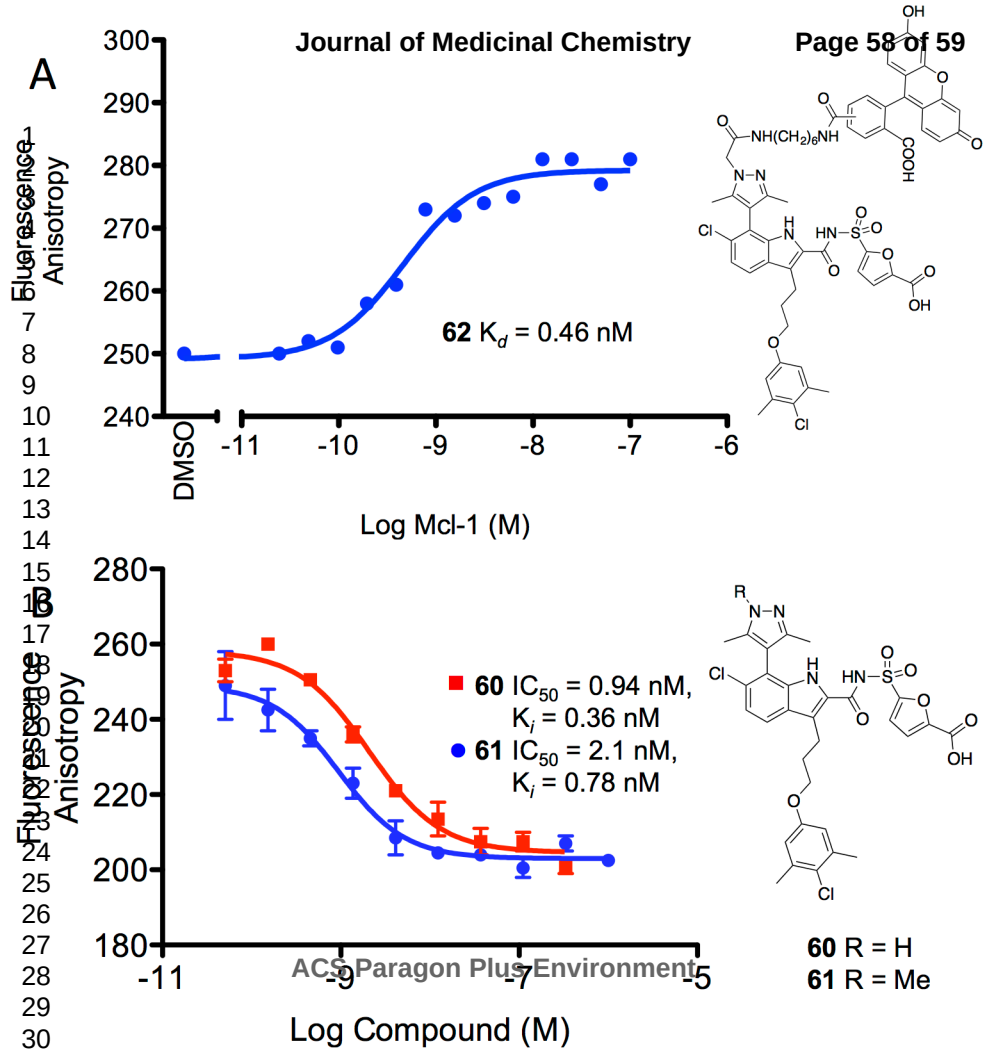
A
Fluorescence Anisotropy
300
290
280
270
260
250
240
DMSO
-11
-10
-9
-8
-7
-6
Log Mcl-1 (M)
62 K_d = 0.46 nM
B
Fluorescence Anisotropy
280
260
240
220
200
180
-11
-9
-7
-5
Log Compound (M)
60 IC_{50} = 0.94 nM, K_i = 0.36 nM
61 IC_{50} = 2.1 nM, K_i = 0.78 nM
60 R = H
61 R = Me